Joint Resource Optimization for Multicell Networks With Wireless Energy Harvesting Relays

Ali Arshad Nasir, *Member, IEEE*, Duy Trong Ngo, *Member, IEEE*, Xiangyun Zhou, *Member, IEEE*, Rodney A. Kennedy, *Fellow, IEEE*, and Salman Durrani, *Senior Member, IEEE*

***Abstract*—This paper first considers a multicell network deployment where the base station (BS) of each cell communicates with its cell-edge user with the assistance of an amplify-and-forward (AF) relay node. Equipped with a power splitter and a wireless energy harvester, the self-sustaining relay scavenges radio-frequency (RF) energy from the received signals to process and forward information. Our aim is to develop a resource allocation scheme that jointly optimizes 1) BS transmit power, 2) received power-splitting factors for energy harvesting and information processing at the relays, and 3) relay transmit power. In the face of strong intercell interference and limited radio resources, we formulate three highly nonconvex problems with the objectives of sum-rate maximization, max-min throughput fairness, and sum-power minimization. To solve such challenging problems, we propose applying the successive convex approximation approach and devising iterative algorithms based on geometric programming and difference-of-convex-function programming. The proposed algorithms transform the nonconvex problems into a sequence of convex problems, each of which is solved very efficiently by the interior-point method. We prove that our algorithms converge to the locally optimal solutions that satisfy the Karush–Kuhn–Tucker (KKT) conditions of the original nonconvex problems. We then extend our results to the case of decode-and-forward (DF) relaying with variable timeslot durations. We show that our resource allocation solutions in this case offer better throughput than that of the AF counterpart with equal timeslot durations, albeit at higher computational complexity. Numerical results confirm that the proposed joint optimization solutions substantially improve network performance, compared with cases where the radio resource parameters are individually optimized.**

***Index Terms*—Convex optimization, multicell interference, resource allocation, successive convex approximation (SCA), wireless energy harvesting.**

Manuscript received August 19, 2014; accepted August 10, 2015. Date of publication August 24, 2015; date of current version August 11, 2016. The work of A. A. Nasir, X. Zhou, and S. Durrani was supported by the Australian Research Council's Discovery Project funding scheme under Project DP140101133. The work of D. T. Ngo was supported by the University of Newcastle's Early Career Researcher Grant G1301282. The review of this paper was coordinated by Prof. J.-M. Chung.

A. A. Nasir is with the School of Electrical Engineering and Computer Science (SEECS), National University of Sciences and Technology (NUST), Islamabad 44000, Pakistan (e-mail: ali.nasir@seecs.nust.edu.pk).

D. T. Ngo is with the School of Electrical Engineering and Computer Science, The University of Newcastle, Callaghan, NSW 2308, Australia (e-mail: duy.ngo@newcastle.edu.au).

X. Zhou, R. A. Kennedy, and S. Durrani are with the Research School of Engineering, Australian National University, Canberra, ACT 2601, Australia (e-mail: xiangyun.zhou@anu.edu.au; rodney.kennedy@anu.edu.au; salman.durrani@anu.edu.au).

Color versions of one or more of the figures in this paper are available online at http://ieeexplore.ieee.org.

Digital Object Identifier 10.1109/TVT.2015.2472295

I. Introduction

MULTICELL networks with universal frequency reuse play an important role in meeting the ever-increasing demand for ubiquitous wireless coverage and high data throughput in the near future [1]–[3]. One of the challenges in such networks is to maintain the quality-of-service (QoS) requirements for cell-edge users due to the interference from the neighboring cells [1], [2]. The deployment of relays is regarded as a viable solution in eliminating coverage holes in areas that are otherwise difficult for base station (BS) signals to penetrate [4], [5]. In addition, the performance of multicell networks can be further enhanced by utilizing coordinated multipoint (CoMP) transmission and reception techniques [6], [7], in which BSs and relays cooperate with one another to best serve the cell-edge users.

Due to random positions and mobility of users, relays need to be opportunistically deployed where they are needed most. This can be achieved if relays do not require a wired power connection and are powered using alternative "green" energy resources. Recently, radio frequency (RF) or wireless energy harvesting has emerged as an attractive solution to power wireless nodes [8]. While energy harvesting from ambient sources may not be sufficient to power relay nodes, carefully designed wireless power transfer links can be used to power relay nodes [8]–[10]. In this regard, it is crucial to ensure that the very different information decoding and power transfer power sensitivity requirements are met at the receiver (e.g., -60 dBm for information receivers and from -10 to -30 dBm for energy receivers [8]).

A multicell network with energy harvesting relays poses interesting design challenges, such as 1) how to effectively manage intercell interference, 2) how to allocate limited power at the BSs, 3) how to design wireless power transfer links for amplify-and-forward (AF) and decode-and-forward (DF) relays, and 4) how the harvested RF energy is utilized at the relays. Existing research in the literature has partially addressed these important issues. The design of wireless energy harvesting relays in point-to-point single-cell systems is considered in [11]–[17]. Assuming simultaneous wireless information and power transfer in a single-cell network, the power control problem for multiuser broadband wireless systems without relays is studied in [18]. In [19], a similar problem is examined, albeit in the context of multiuser multiple-input–multiple-output systems. Considering relays in a single-cell network, resource allocation schemes for the remote radio heads are specifically developed in [20]. In the downlink of a multicell multiuser

interference network, coordinated scheduling and power control algorithms for the macrocell BSs only are proposed in [21] and [22]. Recently, in [23], an optimal power-splitting (PS) rule has been devised for energy harvesting and information processing at the self-sustaining relays of multiuser interference networks. However, in [23], the important issue of allocating the transmit power at the BSs and the relays is not considered.

In this paper, we consider a multicell network in which the BS of each cell communicates with its cell-edge user via a wireless energy harvesting relay node. The relay is equipped with an energy harvesting receiver and an information transceiver. We assume that the energy harvesting receiver implements a PS-based receiver architecture [24], i.e., the relay uses a portion of the received signal power for energy harvesting and the remaining signal energy as input to the information transceiver. Using the harvested energy, the information transceiver employs either AF or DF relaying to forward the received signal to its corresponding user. The BSs in the multicell network adopt CoMP transmission and reception, i.e., they share the channel quality measurements and schedule the transmissions, allowing for more efficient radio resource utilization.

First, we formulate three new resource optimization problems for multicell networks with energy-harvesting-enabled AF relays, namely, sum-rate maximization, minimum-throughput maximization, and sum-power minimization.[1] The objective is to jointly optimize the transmit power at the BSs and the relays and find the optimal PS rule at the relays. Our formulations directly target the critical issue of multicell interference, while meeting the stringent constraints on the available transmit power at the BSs and the relays. Since the optimization variables are strongly coupled with many nonlinear cross-multiplying terms, the formulated problems are highly nonconvex. To the best of our knowledge, there exists no practical method that guarantees true global optimality in these challenging problems.

Then, we exploit the problem structure and adopt the successive convex approximation (SCA) method to transform the highly nonconvex problems into a series of convex subproblems. Here, we specifically tailor the generic SCA framework via the applications of geometric programming (GP) and difference-of-convex-function (DC) programming. At each step in our proposed iterative algorithms, we efficiently solve the resulting convex problem by the interior-point method. We analytically prove that our developed algorithms generate a sequence of improved feasible solutions, which eventually converge to a locally optimal solution satisfying the Karush–Kuhn–Tucker (KKT) conditions of the original problems. Note that the general convergence analysis of the SCA method is established in [26], and SCA-based solutions have been empirically shown to often achieve global optimality in many practical applications, e.g., in wireline DSL networks [27], wireless interference networks [28], [29], and small-cell heterogeneous networks [30].

[1]A preliminary version of this work, which considers the sum-rate maximization problem for AF relaying only, has been accepted for presentation at the 2015 IEEE International Conference on Communications (ICC), London, U.K. [25].

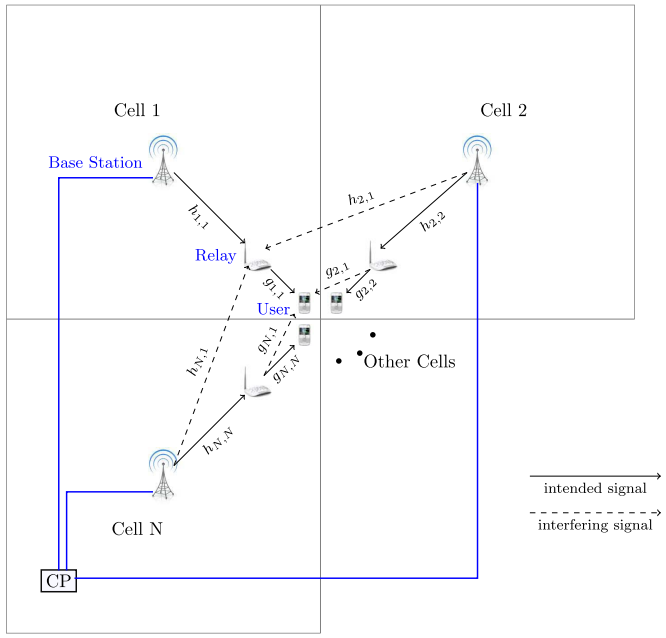

Fig. 1. Multicell network consisting of N cells and a CP unit. Each cell has a BS, a relay, and a cell-edge user. For clarity, we only show the interfering scenarios in Cell 1, i.e., at relay 1 and user 1. In general, interference happens at all N relays and N users.

Finally, we show that the proposed SCA-based approach can be extended to the more general case of variable timeslot durations with DF relaying. Numerical examples with realistic network parameters confirm that our joint optimization solutions significantly outperform those where the radio resource parameters are individually optimized.

The rest of this paper is organized as follows: Section II presents the system model and states the key assumptions used throughout this work. Section III presents the signal model for AF relaying and equal timeslot durations. Section IV formulates the nonconvex resource allocation problems and introduces the generic SCA framework. Sections V and VI propose the GP- and DC-based SCA solutions for AF relaying, respectively. Section VII extends our results to the case of variable timeslot durations with DF relaying. Section VIII presents numerical results to confirm the advantages of our proposed algorithms, and Section IX concludes this paper.

II. System Model and Assumptions

Consider the downlink transmissions in an N-cell network with universal frequency reuse, i.e., the same radio frequencies are used in all cells. Adopting CoMP transmission and reception, we assume that the BSs are connected to a central processing (CP) unit that coordinates the multicellular transmissions and radio resource management. The network under consideration is shown in Fig. 1. Note that although square cells are shown in Fig. 1, the analysis and proposed solutions in this paper are valid for any cellular network geometry.

Let $\mathcal{N} = \{1, \ldots, N\}$ denote the set of all cells. In each cell $i \in \mathcal{N}$, the BS attempts to establish communication with its cell-edge users. We assume that these users are located in the "signal dead zones," where no direct signal from their serving

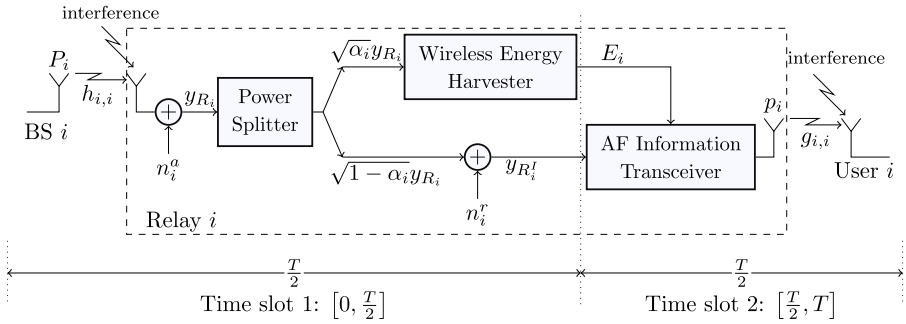

Fig. 2. BS-to-user communication assisted by an RF-powered relay.

BS can be reached. A relay node is deployed in each cell to assist in forwarding the signal from the BS, extending the network coverage to the distant users. We assume that orthogonal channels are assigned to users in each cell (e.g., by means of time-division multiple access, frequency-division multiple access, or orthogonal frequency-division multiple access); hence, intracell interference is eliminated. Therefore, we only focus on the resource allocation in one channel, which corresponds to only one user in a cell. By BS i, relay i, and user i, we mean the BS, the relay, and the single user of cell $i \in \mathcal{N}$, respectively.

We assume that the relays are energy-constrained nodes and that they harvest energy from the RF signals of all BSs, using the PS-based receiver architecture. While each BS has a maximum power limit $P_{\max}$ available for transmission, it must transmit with minimum transmit power $P_{\min}$ to ensure that the energy harvesting circuit at the relay is activated. The harvested energy is used by a relay transceiver to process and forward the BS signal to its intended user. We further assume that the relays are mounted on the building rooftops to have a line-of-sight link from the serving BSs.

Let $h_{i,j}$ be the channel coefficient from BS i to relay j and $g_{j,k}$ be the channel coefficient from relay j to user k. We assume that all the BSs send the available channel state information (CSI) to the CP unit via a dedicated control channel. In this paper, we assume perfect knowledge of CSI at the BSs, allowing for a benchmark performance to be determined.

III. Signal Model With Amplify-and-Forward Relaying

We first consider the case of AF relaying where we divide the total transmission block time T into two equal timeslots. The first timeslot includes BS-to-relay transmissions and energy harvesting at the relays. During the first timeslot, the relays do not transmit. The second timeslot includes signal processing at the relays and relay-to-user transmissions. In this second timeslot, the BSs do not transmit. The operations in each timeslot are shown in Fig. 2, which will be further discussed in the following.

A. BS-to-Relay Transmissions and Wireless Energy Harvesting at Relay Receivers

In the first timeslot $[0, T/2]$, let x_i be the normalized information signal to be sent by BS i, i.e., $\mathbb{E}\{|x_i|^2\} = 1$, where $\mathbb{E}\{\cdot\}$ denotes the expectation operator, and $|\cdot|$ is the absolute value operator. Let $P_{\min} \le P_i \le P_{\max}$ denote the transmit power of BS i, $d_{i,j}^h$ the distance between BS i and relay j, and β the path-loss exponent. Assuming that n_i^a is the zero-mean additive white Gaussian noise (AWGN) with variance σ_i^a at the receiving antenna of relay i, the received signal at relay i can be expressed as

$$y_{R_i} = \frac{h_{i,i}}{\sqrt{\left(d_{i,i}^h\right)^\beta}}\sqrt{P_i}x_i + \sum_{j=1, j\neq i}^{N} \frac{h_{j,i}}{\sqrt{\left(d_{j,i}^h\right)^\beta}}\sqrt{P_j}x_j + n_i^a. \quad (1)$$

We assume that each relay is equipped with a power splitter that determines how much received signal energy should be dedicated to the energy harvester and the signal processing receiver [11], [12], [23], [24]. As shown in Fig. 2, the power splitter at relay $i \in \mathcal{N}$ divides the power of y_{R_i} into two parts in the proportion of $\alpha_i : (1-\alpha_i)$. Here, $\alpha_i \in (0,1)$ is termed as the PS factor. The first part $\sqrt{\alpha_i}y_{R_i}$ is processed by the energy harvester and stored as energy (e.g., by charging a battery at relay i) for the use in the second timeslot. The amount of energy harvested at relay i is given by

$$E_i = \frac{\eta\alpha_i T}{2}\sum_{j=1}^{N} P_j \bar{h}_{j,i} \quad (2)$$

where $\eta \in (0,1)$ is the efficiency of energy conversion, and $\bar{h}_{j,i} \triangleq |h_{j,i}|^2 \left(d_{j,i}^h\right)^{-\beta}\ \forall i,j \in \mathcal{N}$, is the effective channel gain from BS j to relay i (including the effects of both small-scale fading and large-scale path loss).

The second part $\sqrt{1-\alpha_i}y_{R_i}$ of the received signal is passed to an information transceiver. In Fig. 2, n_i^r denotes the AWGN with zero mean and variance σ_i^r introduced by the baseband processing circuitry. Since antenna noise power σ_i^a is very small compared with the circuit noise power σ_i^r in practice [31], n_i^a has a negligible impact on both the energy harvester and the information transceiver of relay i. Thus, for simplicity, we will ignore the effect of n_i^a in the following analysis by setting $\sigma_i^a = 0$. The signal at the input of the information transceiver of relay i can be written as

$$\begin{aligned} y_{R_i}^I &= \sqrt{1-\alpha_i}y_{R_i} + n_i^r \\ &= \sqrt{1-\alpha_i}\frac{h_{i,i}}{\sqrt{\left(d_{i,i}^h\right)^\beta}}\sqrt{P_i}x_i \\ &\quad + \sqrt{1-\alpha_i}\sum_{j=1, j\neq i}^{N}\frac{h_{j,i}}{\sqrt{\left(d_{j,i}^h\right)^\beta}}\sqrt{P_j}x_j + n_i^r \end{aligned} \quad (3)$$

where the first term in (3) is the desired signal from BS i, and the second term is the total interference from all other BSs.

B. Signal Processing at Relays and Relay-to-User Transmissions

In the second timeslot $[T/2, T]$, the information transceiver amplifies the signal $y_{R_i}^I$ prior to forwarding it to user i. Denote the transmit power of relay transceiver i as p_i. With the harvested energy E_i in (55), the maximum power available for transmission at relay i is given by $E_i/(T/2) = 2E_i/T$, which means that

$$p_i \leq \frac{2E_i}{T} = \eta\alpha_i \sum_{j=1}^{N} P_j \bar{h}_{j,i}. \tag{4}$$

The transmitted signal from relay i to user i can then be written as

$$x_{R_i} = \frac{\sqrt{p_i} y_{R_i}^I}{\sqrt{(1-\alpha_i)\sum_{j=1}^{N} P_j \bar{h}_{j,i} + \sigma_i^r}} \tag{5}$$

where the denominator of (5) represents an amplifying factor that ensures power constraint (4) is met.

Now, the received signal at user i is

$$y_{U_i} = \frac{g_{i,i}}{\sqrt{\left(d_{i,i}^g\right)^{\beta}}} x_{R_i} + \sum_{j=1, j\neq i}^{N} \frac{g_{j,i}}{\sqrt{\left(d_{j,i}^g\right)^{\beta}}} x_{R_j} + n_i^u \tag{6}$$

where $d_{i,j}^g$ denotes the distance between relay i and user j, and n_i^u is the AWGN with zero mean and variance σ_i^u at the receiver of user i. Substituting x_{R_i} in (5) into (6) yields

$$y_{U_i} = \frac{g_{i,i}\sqrt{p_i} y_{R_i}^I}{\sqrt{\left(d_{i,i}^g\right)^{\beta}\left[(1-\alpha_i)\sum_{k=1}^{N} P_k \bar{h}_{k,i} + \sigma_i^r\right]}} + \sum_{j=1, j\neq i}^{N} \frac{g_{j,i}\sqrt{p_j} y_{R_j}^I}{\sqrt{\left(d_{i,i}^g\right)^{\beta}\left[(1-\alpha_j)\sum_{k=1}^{N} P_k \bar{h}_{k,j} + \sigma_j^r\right]}} + n_i^u. \tag{7}$$

With $y_{R_i}^I$ defined in (3), we can then write (7) explicitly as

$$y_{U_i} = \frac{g_{i,i} h_{i,i}\sqrt{p_i P_i (1-\alpha_i)} x_i}{\sqrt{\left(d_{i,i}^g d_{i,i}^h\right)^{\beta}\left[(1-\alpha_i)\sum_{k=1}^{N} P_k \bar{h}_{k,i} + \sigma_i^r\right]}}$$

$$+ \frac{g_{i,i}\sqrt{p_i(1-\alpha_i)} \sum_{j=1, j\neq i}^{N} \frac{h_{j,i}}{\sqrt{\left(d_{j,i}^h\right)^{\beta}}} \sqrt{P_j} x_j}{\sqrt{\left(d_{i,i}^g\right)^{\beta}\left[(1-\alpha_i)\sum_{k=1}^{N} P_k \bar{h}_{k,i} + \sigma_i^r\right]}}$$

$$+ \frac{g_{i,i}\sqrt{p_i} n_i^r}{\sqrt{\left(d_{i,i}^g\right)^{\beta}\left[(1-\alpha_i)\sum_{k=1}^{N} P_k \bar{h}_{k,i} + \sigma_i^r\right]}}$$

$$+ \sum_{j=1, j\neq i}^{N} \frac{g_{j,i}\sqrt{p_j} y_{R_j}^I}{\sqrt{\left(d_{j,i}^g\right)^{\beta}\left[(1-\alpha_j)\sum_{k=1}^{N} P_k \bar{h}_{k,j} + \sigma_j^r\right]}} + n_i^u. \tag{8}$$

The first term in (8) represents the desired signal from BS i to its serviced user i, whereas other terms represent intercell interference and noise.

Without loss of generality, let us assume $\sigma_i^r = \sigma_i^u = \sigma$, $\forall i \in \mathcal{N}$. From (8), the signal-to-interference-plus-noise ratio (SINR) at the receiver of user i is given in (9), shown at the bottom of the page, where we define the variables as follows:

$$\phi_1^{i,j} \triangleq \frac{\bar{g}_{i,i}\bar{h}_{j,i}}{\sigma^2};\ \ \phi_2^{i,j} \triangleq \frac{\bar{h}_{j,i}}{\sigma};\ \ \phi_3^{i,j} \triangleq \frac{\bar{g}_{j,i}}{\sigma};\ \ \phi_4^{i,j,k} \triangleq \frac{\bar{g}_{j,i}\bar{h}_{k,i}}{\sigma^2} \tag{10}$$

where $\bar{g}_{j,i} \triangleq |g_{j,i}|^2 (d_{j,i}^g)^{-\beta}$, $\forall i, j \in \mathcal{N}$. For notational convenience, let us also define $\mathbf{P} \triangleq [P_1, \ldots, P_N]^T$, $\mathbf{p} \triangleq [p_1, \ldots, p_N]^T$, and $\boldsymbol{\alpha} \triangleq [\alpha_1, \ldots, \alpha_N]^T$. From (9), the achieved throughput in bits per second per hertz of cell i is given by

$$\tau_i(\mathbf{P}, \mathbf{p}, \boldsymbol{\alpha}) = \frac{1}{2}\log_2(1+\gamma_i). \tag{11}$$

An important observation from (9) and (11) is that by dedicating more received power at relay i for energy harvesting (i.e. increasing α_i), one might actually decrease the end-to-end throughput in cell i. This can be verified upon dividing both the numerator and the denominator of γ_i in (9) by $(1-\alpha_i)$. However, if one opts to decrease α_i, the transmit power available at the information transceiver of relay i will be further limited [see (4)], thus potentially reducing the corresponding data rate τ_i. Similarly, increasing the BS transmit power P_i or the relay transmit power p_i does not necessarily increase the throughput τ_i of cell i. The reason is that P_i and p_i appear in the positive terms in both the numerator and the denominator of γ_i. This suggests the importance of the resource allocation problem in this context, which will be addressed in the following section.

$$\gamma_i = \frac{\phi_1^{i,i} P_i p_i (1-\alpha_i)}{\sum_{j=1, j\neq i}^{N} \phi_1^{i,j} P_j p_i (1-\alpha_i) + \sum_{j=1}^{N}\left(\phi_2^{i,j} P_j (1-\alpha_i) + \phi_3^{i,j} p_j\right) + \sum_{j=1, j\neq i}^{N}\sum_{k=1}^{N} \phi_4^{i,j,k} P_k p_j (1-\alpha_i) + 1} \tag{9}$$

IV. Joint Resource Optimization Problems for Amplify-and-Forward Relaying

In this paper, we aim to devise an optimal tradeoff of all three parameters: transmit power at BSs, i.e., $\mathbf{P}$; transmit power at relays, i.e., $\mathbf{p}$; and PS factor at relays, i.e., $\boldsymbol{\alpha}$, to maximize the performance of the multicell network under consideration. Specifically, we will study the following problems, which jointly optimize $(\mathbf{P}, \mathbf{p}, \boldsymbol{\alpha})$ for three different design objectives.

A. Problem (P1): Sum-Rate Maximization

We assume that $P_{\max}$ is the maximum power available for transmission at each BS. Moreover, $P_{\min}$ is the minimum transmit power required at each BS to ensure the activation of energy harvesting circuitry at the relay. The problem of sum-throughput maximization is formulated as follows:

$$\max_{\mathbf{P},\mathbf{p},\boldsymbol{\alpha}} \quad \sum_{i=1}^{N} \tau_i \tag{12a}$$

$$\text{s.t.} \quad 0 \le \alpha_i \le 1 \quad \forall i \in \mathcal{N} \tag{12b}$$

$$P_{\min} \le P_i \le P_{\max} \quad \forall i \in \mathcal{N} \tag{12c}$$

$$0 \le p_i \le \eta \alpha_i \sum_{j=1}^{N} P_j \bar{h}_{j,i} \quad \forall i \in \mathcal{N}. \tag{12d}$$

In this formulation, (12a) is the total network throughput, whereas (12b) are the constraints for the PS factors for all relays. Furthermore, (12c) and (12d) ensure that the transmit power at the BSs and relays does not exceed the maximum allowable.

B. Problem (P2): Max-Min Throughput Fairness

In Problem (P1), the network sum rate is maximized without any consideration given to the throughput actually achieved by the individual users. It might happen that users with more favorable link conditions are allocated with most of the radio resources, leaving nothing for others to fulfill their bare minimum QoS requirements. The latter includes cell-edge users who are the victims of strong intercell interference. In the following, we formulate a max-min fairness problem where the throughput of the most disadvantaged user is maximized. Thus

$$\max_{\mathbf{P},\mathbf{p},\boldsymbol{\alpha}} \quad \min_{i \in \mathcal{N}} \quad \tau_i \qquad \text{s.t.} \quad (12\text{b})-(12\text{d}). \tag{13a}$$

From the network design perspective, (13) can be regarded as the problem of maximizing a common throughput, i.e.,

$$\max_{\mathbf{P},\mathbf{p},\boldsymbol{\alpha},\tau} \quad \tau \tag{14a}$$

$$\text{s.t.} \quad \tau_i \ge \tau \ge 0 \quad \forall i \in \mathcal{N} \tag{14b}$$

$$(12\text{b})-(12\text{d})$$

where τ is an auxiliary variable that denotes the common throughput.

C. Problem (P3): Sum-Power Minimization

Different from Problems (P1) and (P2), our objective here is to minimize the total transmit power consumption subject to guaranteeing some minimum data throughput $\tau_{\min}$ for each user, i.e.,

$$\min_{\mathbf{P},\mathbf{p},\boldsymbol{\alpha}} \quad \sum_{i=1}^{N} P_i \tag{15a}$$

$$\text{s.t.} \quad \tau_i \ge \tau_{\min} \quad \forall i \in \mathcal{N} \tag{15b}$$

$$(12\text{b})-(12\text{d}).$$

This problem is of particular interest for "green" communications, where one wishes to reduce the environmental impacts of the large-scale deployment of wireless communication networks. At the same time, the performance of all cell-edge users is protected with constraint (15b).

All three problems (P1), (P2), and (P3) are *highly nonconvex* in $(\mathbf{P}, \mathbf{p}, \boldsymbol{\alpha})$ because the throughput τ_i in (11) is highly nonconvex in those variables. Even if we fix $\mathbf{p}$ and $\boldsymbol{\alpha}$ and try to optimize the BS transmit power $\mathbf{P}$ alone, τ_i would still be highly nonconvex in the remaining variable $\mathbf{P}$ due to the cross-cell interference terms. Simultaneously optimizing $\mathbf{P}, \mathbf{p}$ and $\boldsymbol{\alpha}$ will be much more challenging due to the *nonlinearity* introduced by the cross-multiplying terms, e.g., $P_k p_j \alpha_i$ in (9) and $\alpha_i P_j$ in (12d).

To efficiently solve Problems (P1), (P2), and (P3), we propose to adopt the SCA approach [26]–[30], [32] to transform the original nonconvex problems into a sequence of relaxed convex subproblems. The key steps of the generic SCA approach are summarized in Algorithm 1 for our formulated optimization problems. However, in applying the SCA approach, there remain two key questions: 1) How do we perform the approximation in Step 2 in generic Algorithm 1, 2) and given that the approximation is known, how do we prove that the iterative algorithm is convergent to an optimal solution? We will provide the answers for those questions in the following sections. Specifically, we will exploit the structure of the formulated problems to propose two types of approximations, i.e., one based on GP programming and the other on DC programming. We will demonstrate that with the given objective functions and constraints, it is possible to apply both approximations to solve the formulated nonconvex problems under the same SCA framework.

Algorithm 1 Generic SCA Algorithm

1: Initialize with a feasible solution $(\mathbf{P}^{[0]}, \mathbf{p}^{[0]}, \boldsymbol{\alpha}^{[0]})$.
2: At the mth iteration, form a convex subproblem by approximating the nonconcave objective function and constraints of (P1), (P2), and (P3) with some concave function around the previous point $(\mathbf{P}^{[m-1]}, \mathbf{p}^{[m-1]}, \boldsymbol{\alpha}^{[m-1]})$.
3: Solve the resulting convex subproblem to obtain an optimal solution $(\mathbf{P}^{[m]}, \mathbf{p}^{[m]}, \boldsymbol{\alpha}^{[m]})$ at the mth iteration.
4: Update the approximation parameters in Step 2 for the next iteration.
5: Go back to Step 2 and repeat until $(\mathbf{P}, \mathbf{p}, \boldsymbol{\alpha})$ converges.

V. Solutions for Amplify-and-Forward Relaying: Successive Complex Approximation Method Using Geometric Programming

To implement Step 2 in Algorithm 1, here, we will make use of the single condensation approximation method [28] to form a relaxed geometric program (GP), instead of directly solving the nonconvex Problems (P1)–(P3). A GP is expressed in the standard form as [33, p. 161]

$$\min_{\mathbf{y}} \quad f_0(\mathbf{y}) \tag{16a}$$
$$\text{s.t.} \quad f_i(\mathbf{y}) \le 1, \quad i = 1, \ldots, m \tag{16b}$$
$$h_\ell(\mathbf{y}) = 1, \quad \ell = 1, \ldots, M \tag{16c}$$

where $f_i(\mathbf{y}),\ i = 0, \ldots, m$ are posynomials, and $h_\ell(\mathbf{y}),\ \ell = 1, \ldots, M$ are monomials.[2] A GP in standard form is a nonlinear and nonconvex optimization problem because posynomials are not convex functions. However, with a logarithmic change of the variables and multiplicative constants, one can easily turn it into an equivalent nonlinear and convex optimization problem (using the property that the log-sum-exp function is convex) [28], [33].

A. GP-Based Approximated Solution for Problem (P1)

First, we express the objective function in (12a) as

$$\max_{\mathbf{P},\mathbf{p},\boldsymbol{\alpha}} \sum_{i=1}^{N} \frac{1}{2}\log_2(1+\gamma_i) \equiv \max_{\mathbf{P},\mathbf{p},\boldsymbol{\alpha}} \ \log_2 \prod_{i=1}^{N}(1+\gamma_i) \tag{17a}$$
$$\equiv \min_{\mathbf{P},\mathbf{p},\boldsymbol{\alpha}} \ \prod_{i=1}^{N} \frac{1}{1+\gamma_i} \tag{17b}$$

where (17b) follows from (17a) since $\log_2(\cdot)$ is a monotonically increasing function. Upon substituting γ_i in (9)–(17b) and replacing $1-\alpha_i$ by an auxiliary variable t_i, it is shown that Problem (P1) in (12) is equivalent to (18), shown at the bottom of the page, where $\mathbf{t} \triangleq [t_1, \ldots, t_N]^T$.

It can be seen that (18) is not yet in the form of (16) because (18a) and (18d) are not posynomials. For notational convenience, let us define

$$u_i(\mathbf{x}) \triangleq \sum_{j=1, j\neq i}^{N} \phi_1^{i,j} P_j p_i t_i + \sum_{j=1}^{N} \left(\phi_2^{i,j} P_j t_i + \phi_3^{i,j} p_j\right) + \sum_{j=1, j\neq i}^{N} \sum_{k=1}^{N} \phi_4^{i,j,k} P_k p_j t_i + 1 \tag{19}$$

$$v_i(\mathbf{x}) \triangleq \sum_{j=1}^{N} \left(\phi_1^{i,j} P_j p_i t_i + \phi_2^{i,j} P_j t_i + \phi_3^{i,j} p_j\right) + \sum_{j=1, j\neq i}^{N} \sum_{k=1}^{N} \phi_4^{i,j,k} P_k p_j t_i + 1 \tag{20}$$

where $\mathbf{x} = [\mathbf{P}^T, \mathbf{p}^T, \mathbf{t}^T]^T \in \mathbb{R}_+^{3N}$. The objective function in (18a) can then be expressed as

$$\prod_{i=1}^{N} \frac{u_i(\mathbf{x})}{v_i(\mathbf{x})}. \tag{21}$$

Since $u_i(\mathbf{x})$ and $v_i(\mathbf{x})$ are both posynomials, $u_i(\mathbf{x})/v_i(\mathbf{x})$ is not necessarily a posynomial, confirming that (18a) is not a posynomial.

To transform Problem (P1) into a GP of the form in (16), we would like the objective function (21) to be a posynomial. To this end, we propose to apply the single condensation method [28] and approximate $v_i(\mathbf{x})$ with a monomial $\tilde{v}_i(\mathbf{x})$ as follows. Given the value of $\mathbf{x}^{[m-1]}$ at the $(m-1)$th iteration, we apply the arithmetic–geometric mean inequality to lower bound $v_i(\mathbf{x})$ at the mth iteration by a monomial $\tilde{v}_i(\mathbf{x})$ as [28, Lemma 1]

$$\begin{aligned} v_i(\mathbf{x}) &\ge \tilde{v}_i(\mathbf{x}) \\ &\triangleq \prod_{j=1}^{N} \left\{ \left(\frac{v_i\left(\mathbf{x}^{[m-1]}\right) P_j p_i t_i}{P_j^{[m-1]} p_i^{[m-1]} t_i^{[m-1]}} \right)^{\frac{\phi_1^{i,j} P_j^{[m-1]} p_i^{[m-1]} t_i^{[m-1]}}{v_i\left(\mathbf{x}^{[m-1]}\right)}} \right. \\ &\quad \times \left(\frac{v_i(\mathbf{x}^{[m-1]}) P_j t_i}{P_j^{[m-1]} t_i^{[m-1]}} \right)^{\frac{\phi_2^{i,j} P_j^{[m-1]} t_i^{[m-1]}}{v_i\left(\mathbf{x}^{[m-1]}\right)}} \\ &\quad \left. \times \left(\frac{v_i\left(\mathbf{x}^{[m-1]}\right) p_j}{p_j^{[m-1]}} \right)^{\frac{\phi_3^{i,j} p_j^{[m-1]}}{v_i\left(\mathbf{x}^{[m-1]}\right)}} \right\} \end{aligned}$$

[2] A monomial $\hat{q}(\mathbf{y})$ is defined as $\hat{q}(\mathbf{y}) \triangleq c y_1^{\hat{a}_1}\, y_2^{\hat{a}_2}, \ldots, y_n^{\hat{a}_n}$, where $c > 0$, $\mathbf{y} = [y_1, y_2, \ldots, y_n]^T \in \mathbb{R}_{++}^n$, and $\hat{\mathbf{a}} = [\hat{a}_1, \hat{a}_2, \ldots, \hat{a}_n]^T \in \mathbb{R}^n$. A posynomial is a nonnegative sum of monomials [33].

$$\min_{\mathbf{P},\mathbf{p},\boldsymbol{\alpha},\mathbf{t}} \quad \prod_{i=1}^{N} \frac{\sum_{j=1, j\neq i}^{N} \phi_1^{i,j} P_j p_i t_i + \sum_{j=1}^{N} \left(\phi_2^{i,j} P_j t_i + \phi_3^{i,j} p_j\right) + \sum_{j=1, j\neq i}^{N} \sum_{k=1}^{N} \phi_4^{i,j,k} P_k p_j t_i + 1}{\sum_{j=1}^{N} \left(\phi_1^{i,j} P_j p_i t_i + \phi_2^{i,j} P_j t_i + \phi_3^{i,j} p_j\right) + \sum_{j=1, j\neq i}^{N} \sum_{k=1}^{N} \phi_4^{i,j,k} P_k p_j t_i + 1} \tag{18a}$$
$$\text{s.t.} \quad t_i + \alpha_i \le 1, \ \ \forall i \in \mathcal{N} \tag{18b}$$
$$t_i \ge 0, \ \ \forall i \in \mathcal{N} \tag{18c}$$
$$0 \le \frac{p_i}{\eta \alpha_i \sum_{j=1}^{N} P_j \bar{h}_{j,i}} \le 1, \ \ \forall i \in \mathcal{N} \tag{18d}$$
$$(12b),\ (12c)$$

$$\times\ v_i\left(\mathbf{x}^{[m-1]}\right)^{\frac{1}{v_i\left(\mathbf{x}^{[m-1]}\right)}} \times \prod_{j=1,j\neq i}^{N}\prod_{k=1}^{N}\left(\frac{v_i\left(\mathbf{x}^{[m-1]}\right)P_k p_j t_i}{P_k^{[m-1]}p_j^{[m-1]}t_i^{[m-1]}}\right)^{\frac{\phi_4^{i,j,k}P_k^{[m-1]}p_j^{[m-1]}t_i^{[m-1]}}{v_i\left(\mathbf{x}^{[m-1]}\right)}}. \tag{22}$$

It is straightforward to verify that $v_i(\mathbf{x}^{[m-1]}) = \tilde{v}_i(\mathbf{x}^{[m-1]})$. In fact, $\tilde{v}_i(\mathbf{x})$ is the best local monomial approximation to $v_i(\mathbf{x})$ near $\mathbf{x}^{[m-1]}$ in the sense of the first-order Taylor approximation. With (22), the objective function $u_i(\mathbf{x})/v_i(\mathbf{x})$ in (18a) is approximated by $u_i(\mathbf{x})/\tilde{v}_i(\mathbf{x})$. The latter is a posynomial because $\tilde{v}_i(\mathbf{x})$ is a monomial, and the ratio of a posynomial to a monomial is a posynomial. The upper bound $\prod_{i=1}^{N}(u_i(\mathbf{x})/\tilde{v}_i(\mathbf{x}))$ of (21) is also a posynomial because the product of posynomials is a posynomial.

Next, we will approximate constraint (12d) by a posynomial to fit into the GP framework (16). Again, we lower bound posynomial $\eta\alpha_i\sum_{j=1}^{N}P_j\bar{h}_{j,i}$ by a monomial as [28, Lemma 1]

$$\eta\alpha_i\sum_{j=1}^{N}P_j\bar{h}_{j,i} \geq \underbrace{\eta\alpha_i\prod_{j=1}^{N}\left(\frac{P_j\sum_{k=1}^{N}P_k^{[m-1]}\bar{h}_{k,i}}{P_j^{[m-1]}}\right)^{\frac{P_j^{[m-1]}\bar{h}_{j,i}}{\sum_{k=1}^{N}P_k^{[m-1]}\bar{h}_{k,i}}}}_{\triangleq w_i(\alpha_i,\mathbf{P})}. \tag{23}$$

It is clear that the ratio $p_i/w_i(\alpha_i,\mathbf{P})$ is now a posynomial. Upon substituting (22) and (23) into (18), we can formulate an approximated subproblem at the mth iteration for Problem (P1) as follows:

$$\min_{\mathbf{x},\boldsymbol{\alpha}} \quad \prod_{i=1}^{N}\frac{u_i(\mathbf{x})}{\tilde{v}_i(\mathbf{x})} \tag{24a}$$

$$\text{s.t.} \quad 0 \leq \frac{p_i}{w_i(\alpha_i,\mathbf{P})} \leq 1, \ \ \forall i \in \mathcal{N} \tag{24b}$$

$$(12b), (12c), (18b), (18c).$$

Comparing with (16), we see that (24) belongs to the class of a geometric program, i.e., a convex optimization problem. In (24a), since $v_i(\mathbf{x}) \geq \tilde{v}_i(\mathbf{x})$ [see (22)], we are actually minimizing the upper bound of the original objective function in (18a). With (23), constraint (24b) is stricter than (12d) as

$$\frac{p_i}{\eta\alpha_i\sum_{j=1}^{N}P_j\bar{h}_{j,i}} \leq \frac{p_i}{w_i(\alpha_i,\mathbf{P})} \leq 1. \tag{25}$$

B. GP-Based Approximated Solution for Problem (P2)

By substituting τ_i in (11) and carrying out simple algebraic manipulations, constraint (14b) of Problem (P2) can be rewritten as

$$\frac{e^{2\tau\ln 2}}{1+\gamma_i} \leq 1 \ \ \forall i \in \mathcal{N}; \quad \text{and } \tau \geq 0 \tag{26}$$

where $\ln(\cdot)$ denotes the natural logarithm. By introducing the auxiliary variable $\mathbf{t}$ and with $u_i(\mathbf{x})$ and $v_i(\mathbf{x})$ defined in (19) and (20), it is shown that Problem (P2) is equivalent to

$$\max_{\mathbf{x},\boldsymbol{\alpha},\tau} \quad \tau \tag{27a}$$

$$\text{s.t.} \quad \frac{u_i(\mathbf{x})e^{2\tau\ln 2}}{v_i(\mathbf{x})} \leq 1 \ \ \forall i \in \mathcal{N} \tag{27b}$$

$$\tau \geq 0 \tag{27c}$$

$$(12b)-(12d), (18b), (18c).$$

As seen, (27) is not yet in the form of the standard GP (16) because constraints (27b) and (12d) are not posynomials. Using the similar approach in Section V-A, we can transform (27b) and (12d) into posynomials by the approximations in (22) and (23). The resulting subproblem at the mth iteration of Problem (P2) can be expressed in the standard GP form as

$$\max_{\mathbf{x},\boldsymbol{\alpha},\tau} \quad \tau \tag{28a}$$

$$\text{s.t.} \quad \frac{u_i(\mathbf{x})e^{2\tau\ln 2}}{\tilde{v}_i(\mathbf{x})} \leq 1 \ \ \forall i \in \mathcal{N} \tag{28b}$$

$$\tau \geq 0 \tag{28c}$$

$$(12b), (12c), (18b), (18c), (24b)$$

where (28b) follows directly from (27b) by replacing $v_i(\mathbf{x})$ with $\tilde{v}_i(\mathbf{x})$ [in (22)], and (24b) is used in lieu of (12d).

C. GP-Based Approximated Solution for Problem (P3)

By introducing an auxiliary variable $\mathbf{t}$ and applying monomial approximation $\tilde{v}_i(\mathbf{x})$ [in (22)] for $v_i(\mathbf{x})$ [in (20)], we can transform the nonconvex constraint (15b) in Problem (P3) into a posynomial form as

$$\frac{u_i(\mathbf{x})e^{2\tau_{\min}\ln 2}}{\tilde{v}_i(\mathbf{x})} \leq 1. \tag{29}$$

Again, we use (24b) instead of (12d) and arrive at the following GP, which is an approximated problem for Problem (P3) at the mth iteration:

$$\min_{\mathbf{x},\boldsymbol{\alpha}} \quad \sum_{i=1}^{N}P_i \tag{30a}$$

$$\text{s.t.} \quad \frac{u_i(\mathbf{x})e^{2\tau_{\min}\ln 2}}{\tilde{v}_i(\mathbf{x})} \leq 1 \quad \forall i \in \mathcal{N} \tag{30b}$$

$$(12b), (12c), (18b), (18c), (24b).$$

D. Proposed GP-Based SCA Algorithm for Joint Resource Allocation

It should be noted that GP problems (24), (28), and (30) are the convex approximations of the original Problems (P1), (P2), and (P3), respectively. In Algorithm 2, we propose an SCA algorithm in which a (convex) GP is optimally solved at each iteration.

Algorithm 2 Proposed GP-Based SCA Algorithm

1: Initialize $m := 1$.
2: Choose a feasible point $(\mathbf{x}^{[0]} \triangleq (\mathbf{P}^{[0]}, \mathbf{p}^{[0]}, \mathbf{t}^{[0]}); \boldsymbol{\alpha}^{[0]})$.
3: Compute the value of $v_i(\mathbf{x}^{[0]}),\ \forall i \in \mathcal{N}$ according to (20).
4: **repeat**

5: Using $v_i(\mathbf{x}^{[m-1]})$, form the approximate monomial $\tilde{v}_i(\mathbf{x})$ according to (22).
6: Using the interior-point method, solve one GP, i.e., (24) or (28) or (30) to find the mth iteration approximated solution $(\mathbf{x}^{[m]} \triangleq (\mathbf{P}^{[m]}, \mathbf{p}^{[m]}, \mathbf{t}^{[m]}); \boldsymbol{\alpha}^{[m]})$ for Problem (P1) or (P2) or (P3), respectively.
7: Compute the value of $v_i(\mathbf{x}^{[m]})$, $\forall i \in \mathcal{N}$ according to (20).
8: Set $m := m + 1$.
9: **until** Convergence of $(\mathbf{x}, \boldsymbol{\alpha})$ or no further improvement in the objective value (24a) or (28a) or (30a)

Proposition 1: Algorithm 2 generates a sequence of improved feasible solutions that converge to a point $(\mathbf{x}^\star, \boldsymbol{\alpha}^\star)$ satisfying the KKT conditions of the original problems [i.e., Problems (P1)–(P3)].

Proof: We will prove that Proposition 1 holds for the case of GP (24) and its corresponding Problem (P1). The proofs for GP (28) [hence, Problem (P2)] and GP (30) [hence Problem (P3)] are similar and will be omitted. From (23), we have that $p_i/(\eta\alpha_i \sum_{j=1}^N P_j \bar{h}_{j,i}) \le p_i/w_i(\alpha_i, \mathbf{P})$. This means that the optimal solution of the approximated problem (24) always belongs to the feasible set of the original Problem (P1).

Next, since $v_i(\mathbf{x}) \ge \tilde{v}_i(\mathbf{x})\ \forall \mathbf{x} \in \mathbb{R}_+^{3N}$, it follows that:

$$\prod_{i=1}^N \frac{u_i\left(\mathbf{x}^{[m]}\right)}{v_i\left(\mathbf{x}^{[m]}\right)} \le \prod_{i=1}^N \frac{u_i\left(\mathbf{x}^{[m]}\right)}{\tilde{v}_i\left(\mathbf{x}^{[m]}\right)} = \min_{\mathbf{x}} \prod_{i=1}^N \frac{u_i(\mathbf{x})}{\tilde{v}_i(\mathbf{x})} \le \prod_{i=1}^N \frac{u_i\left(\mathbf{x}^{[m-1]}\right)}{\tilde{v}_i\left(\mathbf{x}^{[m-1]}\right)} = \prod_{i=1}^N \frac{u_i\left(\mathbf{x}^{[m-1]}\right)}{v_i\left(\mathbf{x}^{[m-1]}\right)} \quad (31)$$

where the last equality holds because $\tilde{v}_i(\mathbf{x}^{[m-1]}) = v_i(\mathbf{x}^{[m-1]})$. As the actual objective value of Problem (P1) is nonincreasing after every iteration, Algorithm 2 will eventually converge to a point $(\mathbf{x}^\star, \boldsymbol{\alpha}^\star)$.

Finally, it can be verified that

$$\nabla\left(\frac{u_i(\mathbf{x})}{v_i(\mathbf{x})}\right)\Big|_{\mathbf{x}=\mathbf{x}^{[m-1]}} = \nabla\left(\frac{u_i(\mathbf{x})}{\tilde{v}_i(\mathbf{x})}\right)\Big|_{\mathbf{x}=\mathbf{x}^{[m-1]}} \quad (32)$$

$$\nabla\left(\frac{p_i}{\eta\alpha_i \sum_{j=1}^N P_j \bar{h}_{j,i}}\right)\Big|_{\alpha_i=\alpha_i^{[m-1]};\mathbf{P}=\mathbf{P}^{[m-1]}} = \nabla\left(\frac{p_i}{w_i(\alpha_i, \mathbf{P})}\right)\Big|_{\alpha_i=\alpha_i^{[m-1]};\mathbf{P}=\mathbf{P}^{[m-1]}} \quad (33)$$

where ∇ denotes the gradient operator. The results in (32) and (33) imply that the KKT conditions of the original Problem (P1) will be satisfied after the series of approximations involving GP (24) converges to the point $(\mathbf{x}^\star, \boldsymbol{\alpha}^\star)$. This completes the proof. ■

VI. Solutions for Amplify-and-Forward Relaying: Successive Complex Approximation Method Using Difference-of-Convex-Function Programming

A. DC-Based Approximated Solution for Problem (P1)

In the GP-based approach proposed in Section V, we have eliminated the logarithm function in the objective function to form a posynomial [see (17)] and solve the resulting (convex) GP. In the current approach, we propose to keep the logarithm function and rewrite the throughput expression as

$$\begin{aligned}
&\log_2(1+\gamma_i) \\
&= \log_2\left(\sum_{j=1}^N \left(\phi_1^{i,j} P_j p_i (1-\alpha_i) + \phi_2^{i,j} P_j (1-\alpha_i) + \phi_3^{i,j} p_j\right) + \sum_{j=1, j\ne i}^N \sum_{k=1}^N \phi_4^{i,j,k} P_k p_j (1-\alpha_i) + 1\right) \\
&\quad - \log_2\left(\sum_{j=1, j\ne i}^N \phi_1^{i,j} \times P_j p_i (1-\alpha_i) + \sum_{j=1}^N \left(\phi_2^{i,j} P_j (1-\alpha_i) + \phi_3^{i,j} p_j\right) + \sum_{j=1, j\ne i}^N \sum_{k=1}^N \phi_4^{i,j,k} P_k p_j (1-\alpha_i) + 1\right) \\
&= \bar{v}_i(\mathbf{x}) - \bar{u}_i(\mathbf{x}) \qquad (34)
\end{aligned}$$

where we define $\bar{u}_i(\mathbf{x}) \triangleq \log_2(u_i(\mathbf{x}))$ and $\bar{v}_i(\mathbf{x}) \triangleq \log_2(v_i(\mathbf{x}))$ with $u_i(\mathbf{x})$ and $v_i(\mathbf{x})$ given in (19) and (20), respectively. We also recall that $\mathbf{x} = [\mathbf{P}^T, \mathbf{p}^T, \mathbf{t}^T]^T \in \mathbb{R}_+^{3N}$, and $\mathbf{t} = \mathbf{1} - \boldsymbol{\alpha} \in \mathbb{R}_+^N$.

Using the following logarithmic change of variables:

$$\bar{P}_i \triangleq \ln P_i; \quad \bar{p}_i \triangleq \ln p_i; \quad \bar{t}_i \triangleq \ln t_i; \quad \bar{\phi}_1^{i,j} \triangleq \ln \phi_1^{i,j}$$
$$\bar{\phi}_2^{i,j} \triangleq \ln \phi_2^{i,j}; \quad \bar{\phi}_3^{i,j} \triangleq \ln \phi_3^{i,j}; \quad \bar{\phi}_4^{i,j,k} \triangleq \ln \phi_4^{i,j,k} \quad (35)$$

for all $i, j, k \in \mathcal{N}$, we can further write $\bar{u}_i(\cdot)$ and $\bar{v}_i(\cdot)$ in terms of the sums of exponentials in $\bar{\mathbf{x}}$, i.e.,

$$\bar{u}_i(\bar{\mathbf{x}}) = \log_2\left(\sum_{j=1, j\ne i}^N e^{\bar{P}_j + \bar{p}_i + \bar{t}_i + \bar{\phi}_1^{i,j}} + \sum_{j=1}^N \left(e^{\bar{P}_j + \bar{t}_i + \bar{\phi}_2^{i,j}} + e^{\bar{p}_j + \bar{\phi}_3^{i,j}}\right) + \sum_{j=1, j\ne i}^N \sum_{k=1}^N e^{\bar{P}_k + \bar{p}_j + \bar{t}_i + \bar{\phi}_4^{i,j,k}} + 1\right) \quad (36)$$

$$\bar{v}_i(\bar{\mathbf{x}}) = \log_2\left(\sum_{j=1}^N \left(e^{\bar{P}_j + \bar{p}_i + \bar{t}_i + \bar{\phi}_1^{i,j}} + e^{\bar{P}_j + \bar{t}_i + \bar{\phi}_2^{i,j}} + e^{\bar{p}_j + \bar{\phi}_3^{i,j}}\right) + \sum_{j=1, j\ne i}^N \sum_{k=1}^N e^{\bar{P}_k + \bar{p}_j + \bar{t}_i + \bar{\phi}_4^{i,j,k}} + 1\right) \quad (37)$$

where $\bar{\mathbf{x}} \triangleq [\bar{\mathbf{P}}^T, \bar{\mathbf{p}}^T, \bar{\mathbf{t}}^T]^T$, $\bar{\mathbf{P}} \triangleq [\bar{P}_1, \ldots, \bar{P}_N]^T$, $\bar{\mathbf{p}} \triangleq [\bar{p}_1, \ldots, \bar{p}_N]^T$, and $\bar{\mathbf{t}} \triangleq [\bar{t}_1, \ldots, \bar{t}_N]^T$. Since the log-sum-exp function is convex [33], both $\bar{u}_i(\bar{\mathbf{x}})$ and $\bar{v}_i(\bar{\mathbf{x}})$ are convex in $\bar{\mathbf{x}}$. However, their difference $\bar{v}_i(\bar{\mathbf{x}}) - \bar{u}_i(\bar{\mathbf{x}}) = \log_2(1+\gamma_i)$ in (34) is not necessarily concave.

Using the first-order Taylor series expansion around a given point $\bar{\mathbf{x}}^{[m-1]}$, we propose to approximate $\bar{v}_i(\bar{\mathbf{x}})$ by an affine function as follows [29]:

$$\bar{v}_i(\bar{\mathbf{x}}) \approx \bar{v}_i\left(\bar{\mathbf{x}}^{[m-1]}\right) + \left(\nabla \bar{v}_i\left(\bar{\mathbf{x}}^{[m-1]}\right)\right)^T \left(\bar{\mathbf{x}} - \bar{\mathbf{x}}^{[m-1]}\right) \quad (38)$$

where the ℓth element of gradient $\nabla\bar{v}_i(\bar{\mathbf{x}})$ is given by (39), shown at the bottom of the page. With the affine approximation (38) and the convex function $\bar{u}_i(\bar{\mathbf{x}})$, it is clear that the throughput can now be approximated by a concave function as

$$\log_2(1+\gamma_i) \approx \bar{v}_i\left(\bar{\mathbf{x}}^{[m-1]}\right) + \left(\nabla\bar{v}_i\left(\bar{\mathbf{x}}^{[m-1]}\right)\right)^T\left(\bar{\mathbf{x}}-\bar{\mathbf{x}}^{[m-1]}\right) - \bar{u}_i(\bar{\mathbf{x}}). \quad (40)$$

By the variable change, i.e.,

$$\bar{\alpha}_i \triangleq \ln\alpha_i \quad \forall i\in\mathcal{N} \quad (41)$$

and upon denoting $\bar{\boldsymbol{\alpha}} \triangleq [\bar{\alpha}_1,\ldots,\bar{\alpha}_N]^T$, the nonconvex constraint (12d) of Problem (P1) can be rewritten as

$$e^{\bar{p}_i} \le \eta e^{\bar{\alpha}_i}\sum_{j=1}^{N} e^{\bar{P}_j}\bar{h}_{j,i}. \quad (42)$$

Applying the arithmetic–geometric inequality, we have that

$$\sum_{j=1}^{N} e^{\bar{P}_j}\bar{h}_{j,i} \ge \prod_{j=1}^{N}\left(\frac{e^{\bar{P}_j}\bar{h}_{j,i}}{\lambda_{j,i}^{[m-1]}}\right)^{\lambda_{j,i}^{[m-1]}} \quad (43)$$

where $\mathbf{P}^{[m-1]}$ is a fixed point, and

$$\lambda_{j,i}^{[m-1]} \triangleq \frac{e^{\bar{P}_j^{[m-1]}}\bar{h}_{j,i}}{\sum_{k=1}^{N} e^{\bar{P}_j^{[m-1]}}\bar{h}_{k,i}}. \quad (44)$$

As such, (42) can be replaced by a stricter constraint, i.e.,

$$e^{\bar{p}_i} \le \tilde{w}_i(\bar{\alpha}_i,\bar{\mathbf{P}}) \triangleq \eta e^{\bar{\alpha}_i}\prod_{j=1}^{N}\left(\frac{e^{\bar{P}_j}\bar{h}_{j,i}}{\lambda_{j,i}^{[m-1]}}\right)^{\lambda_{j,i}^{[m-1]}} \quad (45)$$

which is equivalent to the following affine constraint:

$$\bar{p}_i - \bar{\alpha}_i - \sum_{j=1}^{N}\lambda_{j,i}^{[m-1]}\bar{P}_j - c_i \le 0 \quad (46)$$

where $c_i \triangleq \ln\eta + \sum_{j=1}^{N}\lambda_{j,i}^{[m-1]}(\ln\bar{h}_{j,i} - \ln\lambda_{j,i}^{[m-1]})$ is a constant.

From (40) and (46), we now have the following convex optimization problem that gives an approximated solution to Problem (P1) at the mth iteration:

$$\max_{\bar{\mathbf{x}},\bar{\boldsymbol{\alpha}}} \quad \sum_{i=1}^{N}\bar{v}_i\left(\bar{\mathbf{x}}^{[m-1]}\right) + \left(\nabla\bar{v}_i\left(\bar{\mathbf{x}}^{[m-1]}\right)\right)^T \times\left(\bar{\mathbf{x}}-\bar{\mathbf{x}}^{[m-1]}\right) - \bar{u}_i(\bar{\mathbf{x}}) \quad (47a)$$

$$\text{s.t.} \quad e^{\bar{t}_i} + e^{\bar{\alpha}_i} \le 1 \quad \forall i\in\mathcal{N} \quad (47b)$$

$$e^{\bar{\alpha}_i} \le 1 \quad \forall i\in\mathcal{N} \quad (47c)$$

$$e^{\bar{t}_i} \le 1 \quad \forall i\in\mathcal{N} \quad (47d)$$

$$P_{\min} \le e^{\bar{P}_i} \le P_{\max} \quad \forall i\in\mathcal{N} \quad (47e)$$

$$\bar{p}_i - \bar{\alpha}_i - \sum_{j=1}^{N}\lambda_{j,i}^{[m-1]}\bar{P}_j - c_i \le 0 \quad (47f)$$

where $\bar{\mathbf{x}}^{[m-1]}$ is known from the $(m-1)$th iteration.

B. DC-Based Approximated Solution for Problems (P2) and (P3)

In this case, we apply the same logarithmic change of variables in (35) and (41). We also make use of the results in (40) and (46) to show that Problem (P2) in (14) is approximated by

$$\max_{\bar{\mathbf{x}},\bar{\boldsymbol{\alpha}},\tau} \quad \tau \quad (48a)$$

$$\text{s.t.} \quad \bar{v}_i\left(\bar{\mathbf{x}}^{[m-1]}\right) + \left(\nabla\bar{v}_i\left(\bar{\mathbf{x}}^{[m-1]}\right)\right)^T\left(\bar{\mathbf{x}}-\bar{\mathbf{x}}^{[m-1]}\right) - \bar{u}_i(\bar{\mathbf{x}}) \ge 2\tau \ge 0 \quad \forall i\in\mathcal{N} \quad (48b)$$

(47b)−(47f).

It is clear that (48) is a convex optimization problem for any given point $\bar{\mathbf{x}}^{[m-1]}$.

By a similar approach, Problem (P3) in (15) can be approximated by the following convex problem:

$$\min_{\bar{\mathbf{x}},\bar{\boldsymbol{\alpha}}} \quad \sum_{i=1}^{N} P_i \quad (49a)$$

$$\text{s.t.} \quad \bar{v}_i\left(\bar{\mathbf{x}}^{[m-1]}\right) + \left(\nabla\bar{v}_i\left(\bar{\mathbf{x}}^{[m-1]}\right)\right)^T\left(\bar{\mathbf{x}}-\bar{\mathbf{x}}^{[m-1]}\right) - \bar{u}_i(\bar{\mathbf{x}}) \ge 2\tau_{\min} \quad \forall i\in\mathcal{N} \quad (49b)$$

(47b)−(47f)

$$\nabla^{(\ell)}\bar{v}_i(\bar{\mathbf{x}}) = \frac{1}{v_i(\bar{\mathbf{x}})\ln 2} \times \begin{cases} e^{\bar{P}_\ell+\bar{p}_i+\bar{t}_i+\bar{\phi}_1^{i,\ell}} + e^{\bar{P}_\ell+\bar{t}_i+\bar{\phi}_2^{i,\ell}} + \sum_{j=1,j\ne i}^{N} e^{\bar{P}_\ell+\bar{p}_j+\bar{t}_i+\bar{\phi}_4^{i,j,\ell}}, & \text{if } \ell\in\{1,\ldots,N\} \\ e^{\bar{p}_i+\bar{\phi}_3^{i,i}} + \sum_{j=1}^{N} e^{\bar{P}_j+\bar{p}_i+\bar{t}_i+\bar{\phi}_1^{i,j}}, & \text{if } \ell = N+i \\ e^{\bar{p}_{\ell-N}+\bar{\phi}_3^{i,\ell-N}} + \sum_{k=1}^{N} e^{\bar{P}_k+\bar{p}_{\ell-N}+\bar{t}_i+\bar{\phi}_4^{i,\ell-N,k}}, & \text{if } \ell\in\{N+1,\ldots,2N\}\setminus\{N+i\} \\ \sum_{j=1}^{N}\left(e^{\bar{P}_j+\bar{p}_i+\bar{t}_i+\bar{\phi}_1^{i,j}} + e^{\bar{P}_j+\bar{t}_i+\bar{\phi}_2^{i,j}}\right) + \sum_{j=1,j\ne i}^{N}\sum_{k=1}^{N} e^{\bar{P}_k+\bar{p}_j+\bar{t}_i+\bar{\phi}_4^{i,j,k}}, & \text{if } \ell = 2N+i \\ 0, & \text{otherwise.} \end{cases} \quad (39)$$

where $\bar{\mathbf{x}}^{[m-1]}$ is known from the $(m-1)$th iteration.

C. Proposed DC-Based SCA Algorithm for Joint Resource Allocation

In Algorithm 3, we propose an SCA algorithm in which a convex problem based on the DC approximation is optimally solved at each iteration.

Algorithm 3 Proposed DC-Based SCA Algorithm

1: Initialize $m := 1$.
2: Choose a feasible point $(\mathbf{x}^{[0]} \triangleq (\mathbf{P}^{[0]}, \mathbf{p}^{[0]}, \mathbf{t}^{[0]}); \boldsymbol{\alpha}^{[0]})$ and evaluate $(\bar{\mathbf{x}}^{[0]} \triangleq (\bar{\mathbf{P}}^{[0]}, \bar{\mathbf{p}}^{[0]}, \bar{\mathbf{t}}^{[0]}); \bar{\boldsymbol{\alpha}}^{[0]})$ using (35) and (41).
3: Compute $\bar{v}_i(\bar{\mathbf{x}}^{[0]})$, $\nabla \log_2 \bar{v}_i(\bar{\mathbf{x}}^{[0]})$ and $\lambda_{j,i}^{[0]}$ $\forall i, j \in \mathcal{N}$ using (37), (39), and (44), respectively.
4: **repeat**
5: Given $\bar{v}_i(\bar{\mathbf{x}}^{[m-1]})$, $\nabla \log_2 \bar{v}_i(\bar{\mathbf{x}}^{[m-1]})$ and $\lambda_{j,i}^{[m-1]}$, form one convex problem, i.e., (47) or (48) or (49).
6: Using the interior-point method to solve (47) or (48) or (49) for an approximated solution $(\bar{\mathbf{x}}^{[m]} \triangleq (\bar{\mathbf{P}}^{[m]}, \bar{\mathbf{p}}^{[m]}, \bar{\mathbf{t}}^{[m]}); \bar{\boldsymbol{\alpha}}^{[m]})$ of Problem (P1) or (P2) or (P3) at the mth iteration, respectively.
7: Update $\bar{v}_i(\bar{\mathbf{x}}^{[m]})$, $\nabla \log_2 \bar{v}_i(\bar{\mathbf{x}}^{[m]})$ and $\lambda_{j,i}^{[m]}$ $\forall i, j \in \mathcal{N}$ using (37), (39), and (44), respectively.
8: Set $m := m + 1$.
9: **until** Convergence of $(\bar{\mathbf{x}}, \bar{\boldsymbol{\alpha}})$ or no further improvement in the objective value (47a) or (48a) or (49a)
10: Recover the optimal solution $(\mathbf{x}^\star; \boldsymbol{\alpha}^\star)$ from $(\bar{\mathbf{x}}^\star; \bar{\boldsymbol{\alpha}}^\star)$ via (35) and (41).

Proposition 2: Algorithm 3 generates a sequence of improved feasible solutions that converge to a point $(\mathbf{x}^\star; \boldsymbol{\alpha}^\star)$ satisfying the KKT conditions of the original problems [i.e., Problems (P1)–(P3)].

Proof: We will prove that Proposition 2 holds for the case of (47) and its corresponding Problem (P1). The proofs for (48) [hence, Problem (P2)] and (49) [hence, Problem (P3)] are similar and will be omitted. From (43), we have that $e^{\bar{p}_i} / (\eta e^{\bar{\alpha}_i} \sum_{j=1}^{N} e^{\bar{P}_j} \bar{h}_{j,i}) \leq e^{\bar{p}_i} / \tilde{w}_i(\bar{\alpha}_i, \bar{\mathbf{P}})$. Imposing a stricter constraint means that the optimal solution of the approximated problem (47) always belongs to the feasible set of the original Problem (P1).

Because the gradient of the convex function $\bar{v}_i(\bar{\mathbf{x}})$ is its subgradient [33], it follows that $\forall \mathbf{x} \in \mathbb{R}_+^{3N}$:

$$\bar{v}_i(\bar{\mathbf{x}}) \geq \bar{v}_i\left(\bar{\mathbf{x}}^{[m-1]}\right) + \left(\nabla \bar{v}_i\left(\bar{\mathbf{x}}^{[m-1]}\right)\right)^T \left(\bar{\mathbf{x}} - \bar{\mathbf{x}}^{[m-1]}\right). \quad (50)$$

We now have the following relations for the approximated objective value (47a) at the mth iteration:

$$\begin{aligned}
&\sum_{i=1}^{N} \bar{v}_i\left(\bar{\mathbf{x}}^{[m]}\right) - \bar{u}_i\left(\bar{\mathbf{x}}^{[m]}\right) \\
&\quad \geq \sum_{i=1}^{N} \bar{v}_i\left(\bar{\mathbf{x}}^{[m-1]}\right) + \left(\nabla \bar{v}_i^T\left(\bar{\mathbf{x}}^{[m-1]}\right)\right)^T \\
&\qquad \times \left(\bar{\mathbf{x}}^{[m]} - \bar{\mathbf{x}}^{[m-1]}\right) - \bar{u}_i\left(\bar{\mathbf{x}}^{[m]}\right) \\
&\quad = \max_{\bar{\mathbf{x}}} \sum_{i=1}^{N} \bar{v}_i\left(\bar{\mathbf{x}}^{[m-1]}\right) + \left(\nabla \bar{v}_i^T\left(\bar{\mathbf{x}}^{[m-1]}\right)\right)^T \\
&\qquad \times \left(\bar{\mathbf{x}} - \bar{\mathbf{x}}^{[m-1]}\right) - \bar{u}_i(\bar{\mathbf{x}}) \\
&\quad \geq \sum_{i=1}^{N} \bar{v}_i\left(\bar{\mathbf{x}}^{[m-1]}\right) + \left(\nabla \bar{v}_i^T\left(\bar{\mathbf{x}}^{[m-1]}\right)\right)^T \\
&\qquad \times \left(\bar{\mathbf{x}}^{[m-1]} - \bar{\mathbf{x}}^{[m-1]}\right) - \bar{u}_i\left(\bar{\mathbf{x}}^{[m-1]}\right) \\
&\quad = \sum_{i=1}^{N} \bar{v}_i\left(\bar{\mathbf{x}}^{[m-1]}\right) - \bar{u}_i\left(\bar{\mathbf{x}}^{[m-1]}\right). \quad (51)
\end{aligned}$$

It is clear that the actual objective value of Problem (P1) is nondecreasing after every iteration. Therefore, Algorithm 3 will eventually converge to a point $(\mathbf{x}^\star; \boldsymbol{\alpha}^\star) = (e^{\bar{\mathbf{x}}^\star}; e^{\bar{\boldsymbol{\alpha}}^\star})$.

Finally, it can be verified that

$$\begin{aligned}
&\nabla \left(\bar{v}_i(\bar{\mathbf{x}}) - \bar{u}_i(\bar{\mathbf{x}})\right)\big|_{\bar{\mathbf{x}}=\bar{\mathbf{x}}^{[m-1]}} \\
&\quad = \nabla \left(\bar{v}_i\left(\bar{\mathbf{x}}^{[m-1]}\right) + \left(\nabla \bar{v}_i\left(\bar{\mathbf{x}}^{[m-1]}\right)\right)^T \right. \\
&\qquad \left. \times \left(\bar{\mathbf{x}} - \bar{\mathbf{x}}^{[m-1]}\right) - \bar{u}_i(\bar{\mathbf{x}}) \right)\Big|_{\bar{\mathbf{x}}=\bar{\mathbf{x}}^{[m-1]}} \quad (52) \\
&\nabla \left(\frac{e^{\bar{p}_i}}{\eta e^{\bar{\alpha}_i} \sum_{j=1}^{N} e^{\bar{P}_j} \bar{h}_{j,i}} \right)\Bigg|_{\substack{\bar{\alpha}_i=\bar{\alpha}_i^{[m-1]} \\ \bar{\mathbf{P}}=\bar{\mathbf{P}}^{[m-1]}}} \\
&\quad = \nabla \left(\frac{e^{\bar{p}_i}}{\tilde{w}_i(\bar{\alpha}_i, \bar{\mathbf{P}})} \right)\Bigg|_{\substack{\bar{\alpha}_i=\bar{\alpha}_i^{[m-1]} \\ \bar{\mathbf{P}}=\bar{\mathbf{P}}^{[m-1]}}}. \quad (53)
\end{aligned}$$

The results in (52) and (53) imply that the KKT conditions of the original Problem (P1) will be satisfied after the series of approximations involving convex problem (47) converges to $(\bar{\mathbf{x}}^\star; \bar{\boldsymbol{\alpha}}^\star)$. This completes the proof. ■

Remark 1: As discussed in Sections V and VI, we use the SCA framework to propose two different methods, i.e., GP and DC programming, to solve the three problems (P1)–(P3). In this remark, we present the computational complexity of the two solutions. We first use the big-$\mathcal{O}$ notation to find the computational complexity of the convex subproblems in an iteration [34]. To solve Problem (P1), the complexity of solving both convex subproblems (24) (in Algorithm 2) and (47) (in Algorithm 3) is $\mathcal{O}((4N)^3 5N)$ because they both have $4N$ optimizing variables and $5N$ constraints. Multiplying this factor by the number of iterations required for convergence, we can obtain the overall computational complexity of Algorithms 2 and 3. This implies that the order of complexity for both proposed algorithms is the same. Second, to compare the exact computational time for the proposed algorithms, we evaluate the CPU execution time [35]. For a fair comparison, the MATLAB codes of the two algorithms are optimized to run on the same computer equipped with Intel Core i7-2670QM, a 2.20-GHz processor, and 8 GB of RAM. We have observed that the GP-based algorithm is slightly more efficient than the DC-based algorithm, e.g., in solving Problem (P1), Algorithms 2 and 3, on average, require 29 and 31.5 s, respectively.

VII. System Model and Proposed Solution for Decode-and-Forward Relaying With Variable Timeslot Durations

Here, we extend our work to DF relaying. With DF relaying, we have the flexibility to vary the time duration of BS-to-relay and relay-to-user transmissions. In what follows, we will discuss the signal model, the sum-rate maximization problem with a GP-based solution, and the corresponding complexity analysis for DF relaying.

A. Signal Model

Let ϵT define the fraction of the block time used for relay-to-user transmissions. The remaining block time $(1-\epsilon)T$ is used for BS-to-relay energy harvesting and information transmissions. With the signal at the input of information transceiver at relay i in (3), the SINR at the receiver of relay i is given by

$$\gamma_i^{\mathrm{DF-R}} = \frac{(1-\alpha_i)\bar{h}_{i,i}P_i}{(1-\alpha_i)\sum_{j=1,j\neq i}^{N}\bar{h}_{j,i}P_j+\sigma}. \tag{54}$$

The amount of energy harvested at DF relay i is then

$$E_i = \eta\alpha_i(1-\epsilon)T\sum_{j=1}^{N}P_j\bar{h}_{j,i}. \tag{55}$$

The maximum power available for transmission at DF relay i is $E_i/\epsilon T$, which means that

$$p_i \leq \frac{E_i}{\epsilon T} = \eta\alpha_i\frac{1-\epsilon}{\epsilon}\sum_{j=1}^{N}P_j\bar{h}_{j,i}. \tag{56}$$

DF relay i will decode the signal from BS i and forward it to user i. Let $\bar{x}_i$ be the decoded version of signal x_i sent by BS i. The received signal at user i in DF relaying is

$$y_{U_i} = \frac{g_{i,i}}{\sqrt{\left(d_{i,i}^{g}\right)^{\beta}}}\sqrt{p_i}\bar{x}_i + \sum_{j=1,j\neq i}^{N}\frac{g_{j,i}}{\sqrt{\left(d_{j,i}^{g}\right)^{\beta}}}\sqrt{p_j}\bar{x}_j + n_i^a. \tag{57}$$

The SINR at the receiver of user i is thus

$$\gamma_i^{\mathrm{DF-U}} = \frac{\bar{g}_{i,i}p_i}{\sum_{j=1,j\neq i}^{N}\bar{g}_{j,i}p_j+\sigma}. \tag{58}$$

The achievable throughput in bits per second per hertz of cell i is then given by

$$\tau_i^{\mathrm{DF}}(\mathbf{P},\mathbf{p},\boldsymbol{\alpha},\epsilon) = \epsilon\log_2\left(1+\gamma_i^{\mathrm{DF}}\right) \tag{59}$$

where $\gamma_i^{\mathrm{DF}} \triangleq \min\{\gamma_i^{\mathrm{DF-R}},\gamma_i^{\mathrm{DF-U}}\}$.

B. Sum-Rate Maximization Problem and GP-Based Solution

The problem of sum-throughput maximization for DF relaying is formulated as follows:

$$\max_{\mathbf{P},\mathbf{p},\boldsymbol{\alpha},\epsilon} \quad \epsilon\sum_{i=1}^{N}\log_2\left(1+\min\left\{\gamma_i^{\mathrm{DF-R}},\gamma_i^{\mathrm{DF-U}}\right\}\right) \tag{60a}$$

$$\text{s.t.} \quad 0\leq\alpha_i\leq 1 \quad \forall i\in\mathcal{N} \tag{60b}$$

$$P_{\min}\leq P_i\leq P_{\max} \quad \forall i\in\mathcal{N} \tag{60c}$$

$$0\leq p_i\leq\eta\alpha_i\frac{1-\epsilon}{\epsilon}\sum_{j=1}^{N}P_j\bar{h}_{j,i} \quad \forall i\in\mathcal{N} \tag{60d}$$

$$0\leq\epsilon\leq 1. \tag{60e}$$

We will now demonstrate that the GP-based SCA approach can be used to solve the nonconvex problem (60).[3] To transform problem (60) into a GP of the form in (16), we first fix ϵ to find the optimal solution of other parameters and then optimize ϵ later. By introducing a new auxiliary variable z_i, problem (60) is equivalently expressed as

$$\max_{\mathbf{P},\mathbf{p},\boldsymbol{\alpha},\mathbf{z}} \quad \bar{\epsilon}\sum_{i=1}^{N}\log_2(1+z_i) \tag{61a}$$

$$\text{s.t.} \quad \gamma_i^{\mathrm{DF-R}}\geq z_i \quad \forall i\in\mathcal{N} \tag{61b}$$

$$\gamma_i^{\mathrm{DF-U}}\geq z_i \quad \forall i\in\mathcal{N} \tag{61c}$$

$$0\leq p_i\leq\eta\alpha_i\frac{1-\bar{\epsilon}}{\bar{\epsilon}}\sum_{j=1}^{N}P_j\bar{h}_{j,i} \quad \forall i\in\mathcal{N} \tag{61d}$$

$$(60\text{b}),(60\text{c})$$

where $\mathbf{z}\triangleq[z_1,\ldots,z_N]^T$. The objective function in (61a) is rewritten as

$$\max_{\mathbf{P},\mathbf{p},\boldsymbol{\alpha},\mathbf{z}} \quad \bar{\epsilon}\sum_{i=1}^{N}\log_2(1+z_i) \equiv \min_{\mathbf{P},\mathbf{p},\boldsymbol{\alpha},\mathbf{z}} \quad \prod_{i=1}^{N}\frac{1}{1+z_i}. \tag{62}$$

Next, we approximate the expression $1/(1+z_i)$ in (62) by a posynomial to fit into the GP framework (16). To this end, we lower bound $1+z_i$ by a monomial as [28, Lemma 1]

$$1+z_i \geq \left(1+z_i^{[m-1]}\right)^{\frac{1}{1+z_i^{[m-1]}}} \times\left(\frac{\left(1+z_i^{[m-1]}\right)z_i}{z_i^{[m-1]}}\right)^{\frac{z_i^{[m-1]}}{1+z_i^{[m-1]}}}. \tag{63}$$

By using (62) and (63) and ignoring the constant terms, we further reduce (62) to

$$\equiv \min_{\mathbf{P},\mathbf{p},\boldsymbol{\alpha},\mathbf{z}} \quad \prod_{i=1}^{N}z_i^{-\frac{z_i^{[m-1]}}{1+z_i^{[m-1]}}}. \tag{64}$$

Upon substituting $\gamma_i^{\mathrm{DF-R}}$ and $\gamma_i^{\mathrm{DF-U}}$ from (54) and (58) into (61), replacing $1-\alpha_i$ by an auxiliary variable t_i, applying arithmetic–geometric mean inequality to lower bound $1+z_i$ and $\sum_{j=1}^{N}P_j\bar{h}_{j,i}$ in (62) and (60d) by monomials, we can

[3] Note that the other problems, i.e., max-min throughput and sum-power minimization, can be similarly formulated and solved for DF relaying. For brevity, they are not presented here.

formulate an approximated subproblem at the mth iteration for problem (60) as follows:

$$\min_{\mathbf{P},\mathbf{p},\boldsymbol{\alpha},\mathbf{t},\mathbf{z}} \quad \prod_{i=1}^{N} z_i^{-\frac{z_i^{[m-1]}}{1+z_i^{[m-1]}}} \tag{65a}$$

$$\text{s.t.} \quad \frac{z_i\left(t_i\sum_{j=1,j\neq i}^{N}\bar{h}_{j,i}P_j+\sigma\right)}{t_i\bar{h}_{i,i}P_i} \leq 1 \quad \forall i\in\mathcal{N} \tag{65b}$$

$$\frac{z_i\left(\sum_{j=1,j\neq i}^{N}\bar{g}_{j,i}p_j+\sigma\right)}{\bar{g}_{i,i}p_i} \leq 1 \quad \forall i\in\mathcal{N} \tag{65c}$$

$$0 \leq \frac{\bar{\epsilon}p_i}{(1-\bar{\epsilon})w_i(\alpha_i,\mathbf{P})} \leq 1 \quad \forall i\in\mathcal{N} \tag{65d}$$

$$0 \leq t_i \leq 1 \quad \forall i\in\mathcal{N} \tag{65e}$$

$$\alpha_i + t_i \leq 1 \quad \forall i\in\mathcal{N} \tag{65f}$$

$$(60b), (60c)$$

where

$$w_i(\alpha_i,\mathbf{P}) \triangleq \eta\alpha_i\prod_{j=1}^{N}\left(\frac{P_j\sum_{k=1}^{N}P_k^{[m-1]}\bar{h}_{k,i}}{P_j^{[m-1]}}\right)^{\frac{P_j^{[m-1]}\bar{h}_{j,i}}{\sum_{k=1}^{N}P_k^{[m-1]}\bar{h}_{k,i}}}$$

is defined in (23). Compared with (16), problem (65) belongs to the class of geometric programs, i.e., a convex optimization problem. The convergence of the iterative algorithms that solves convex subproblem (65) for DF relaying can be proved using similar steps as stated in Proposition 1.

Using the optimized values of $\mathbf{P}$, $\mathbf{p}$, and $\boldsymbol{\alpha}$, we have to optimize the time fraction ϵ in the original problem (60). Although (60) is linear in ϵ, constraint (60d) is met with equality at convergence. No further improvement of ϵ can be achieved by solving (60) with the optimized values of $\mathbf{P}$, $\mathbf{p}$, and $\boldsymbol{\alpha}$. Moreover, constraint (60d) is not monotonic in ϵ. Hence, the only available option is to apply exhaustive search to find the optimal value of ϵ in (60) for given optimized values of $\mathbf{P}$, $\mathbf{p}$, and $\boldsymbol{\alpha}$.

Remark 2: In the numerical results in Section VIII, we will show that DF relaying with an optimized timeslot fraction results in more than twice the throughput that is otherwise achieved by AF relaying with equal timeslot durations. However, this performance improvement is at the expense of much higher computational complexity due to the required exhaustive search.

VIII. Numerical Results

Fig. 3 shows an example multicell network consisting of four 150 m × 150 m cells. In each cell, the geographical distance between the servicing BS and its corresponding relay and that between the relay and the cell-edge user is both $35\sqrt{2} \approx 49.5$ m, i.e., the relay in each cell is located midway between the BS and the cell-edge user. At the relays, we set the energy harvesting efficiency to $\eta = 0.5$.[4] To model the wireless channels, we assume independently and identically distributed block fading. Channel coefficients $h_{i,j}$ and $g_{\bar{j},k}$ $\forall i,j,\bar{j},k$ and $i\neq j$, are circularly symmetric complex Gaussian random variables with zero mean and unit variance. The channel coefficients between the servicing BS and its corresponding relay, i.e., $h_{i,i}$ $\forall\, i$, are modeled by Rician fading with the Rician factor of 10 dB. We assume that the randomly generated values of $h_{i,j}$ and $g_{j,k}$ remain unchanged during each time block where the radio resource allocation process takes place. To model large-scale fading, we assume that the path-loss exponent is $\beta = 3$. This results in a maximum path loss of 51 dB between the BS and the associated relay in each cell. To activate RF energy harvesting with $\eta = 0.5$ and assuming that the input power at the energy harvesting relay has to be greater than -25 dBm [8], [36],[5] we set $P_{\min} = -25 + 51 = 26$ dBm. Using a channel bandwidth of 20 kHz and assuming a noise power density of -174 dBm/Hz, the total noise power is calculated as $\sigma = -131$ dBm [37]. We initialize the proposed Algorithms 2 and 3 with $P_i^{[0]} = \varsigma P_{\max}$; $\alpha_i^{[0]} = \varsigma$; $t_i^{[0]} = 1-\alpha_i^{[0]}$; $p_i^{[0]} = \varsigma\eta\alpha_i^{[0]}\sum_{j=1}^{N}P_j^{[0]}\bar{h}_{j,i}$ $\forall i\in\mathcal{N}$, where ς is a real number taken between 0 and 1. To solve each convex problem in Algorithms 2 and 3, we use CVX, which is a package for specifying and solving convex programs [38], [39].

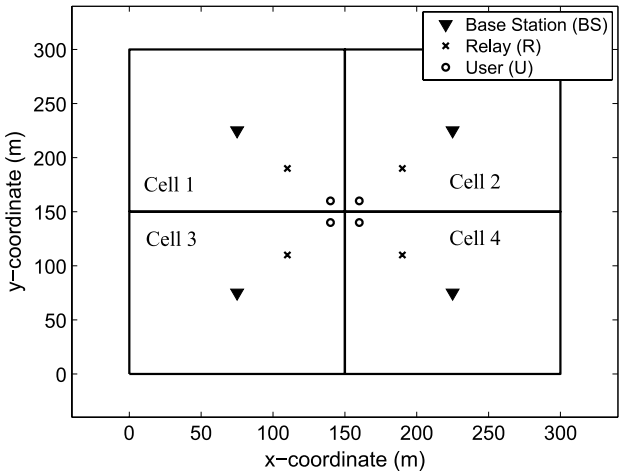

Fig. 3. Topology of the multicell network used in the numerical examples.

A. Convergence of the Proposed Algorithms for AF Relaying

Here, we present numerical results to demonstrate the convergence behavior of the proposed algorithms under different parameter settings. Regarding Problem (P1), Fig. 4 plots the convergence of the sum throughput $\sum_{i=1}^{N}\tau_i$ by the proposed solutions. In our simulations, each iteration corresponds to solving of a GP (24) in Algorithm 2 or a DC program (47) in Algorithm 3 by CVX. It is clear from Fig. 4 that both algorithms exhibit similar convergence behaviors. In our example, they converge within 15 iterations and achieve the same optimal throughput. As observed from Fig. 4(a), the sum rate

[4]The value of η is typically in the range of 0.4–0.6 for practical energy harvesting circuits [8].

[5]Energy conversion efficiency of around 50% has been reported in the ISM band (900 MHz, 2.4 GHz) with an RF input power of -25 dBm and using 13-nm CMOS technology [8], [36].

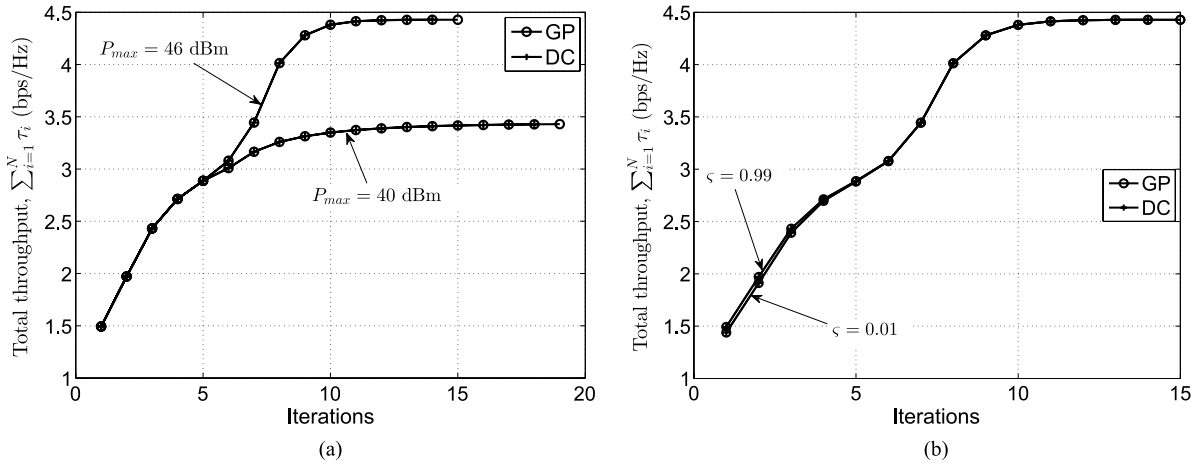

Fig. 4. Convergence of Algorithms 2 and 3 in Problem (P1) for AF relaying. (a) Fixed $\varsigma = 0.5$. (b) Fixed $P_{\max} = 46$ dBm.

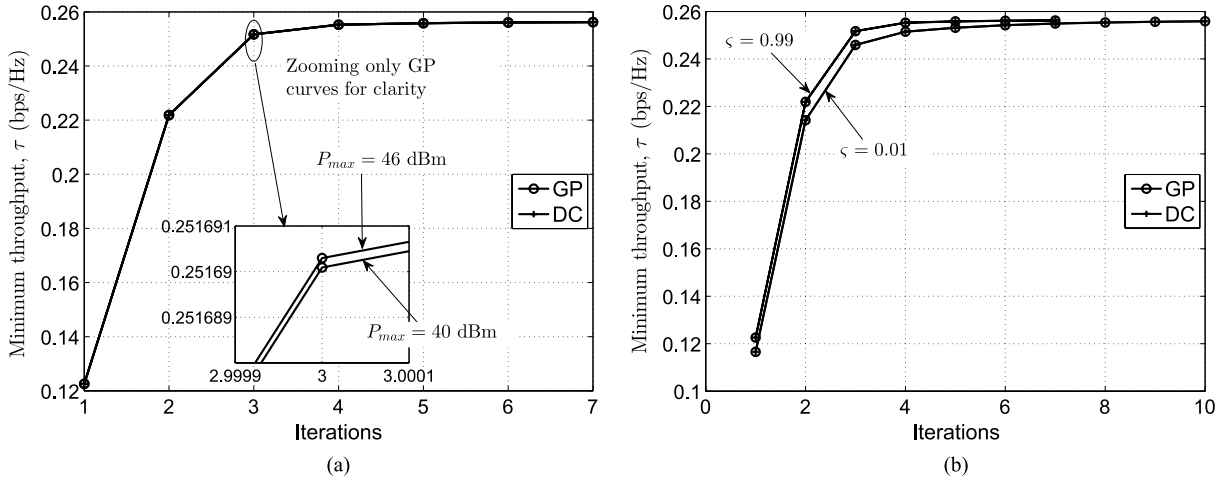

Fig. 5. Convergence of Algorithms 2 and 3 in Problem (P2) for AF relaying. (a) Fixed $\varsigma = 0.5$. (b) Fixed $P_{\max} = 46$ dBm.

is increased by 28% if we allow a higher BS transmit power budget of 46 dBm instead of 40 dBm. In an interference-limited multicell multiuser network setting, increasing the transmit power may trigger the "power racing" phenomenon among the users, which, in turn, adversely affect the total achieved throughput. Our numerical results, on the other hand, confirm that the proposed algorithms effectively manage the strong intercell interference and maximize the network performance. For a fixed power budget $P_{\max} = 46$ dBm, Fig. 4(b) demonstrates that the final performance of our algorithms is insensitive to the initial points, further suggesting that the solution corresponds to the actual global optimum in our example [27]–[29].

We demonstrate the performance of our developed algorithms in Figs. 5 and 6 for Problems (P2) and (P3), respectively, which plot the convergence of the minimum throughput τ and total BS transmit power $\sum_{i=1}^{N} P_i$, respectively. Again, the proposed algorithms quickly converge to the corresponding optimal values. Different from the results for Problem (P1), increasing $P_{\max}$ from 40 to 46 dBm in Fig. 5(a) marginally improves the achieved minimum throughput. This signifies the challenge of enhancing the performance of the most disadvantaged user, who is typically located in the cell-edge areas and suffers from strong intercell interference. In this situation, simply increasing the total allowable transmit power at the BSs would not be helpful. On the other hand, Fig. 6(a) verifies that the total required transmit power drops to the minimum value possible, i.e., $N \times P_{\min} = 32$ dBm for different values of minimum throughput. Similar to Figs. 4(b), 5(b) and 6(b) show that initializing the algorithms with different values of ς, again, does not affect the final solutions.

As shown in Figs. 4–6, both Algorithms 2 and 3 achieve the same optimal values. However, it is impractical to compare their performance with a globally optimal solution. There is no global optimization approach available in the literature to solve our highly nonconvex optimization problems. A direct exhaustive search would incur prohibitive computational complexity. It is noteworthy that in [27]–[29], it is shown that the SCA approach often empirically achieves global optimality in most practical network applications. Moreover, since we assume perfect knowledge of CSI at the BSs, the achieved performance corresponds to the theoretical bound that can be obtained. The actual performance with channel estimation errors is out of the scope of this work and is a potential future research direction.

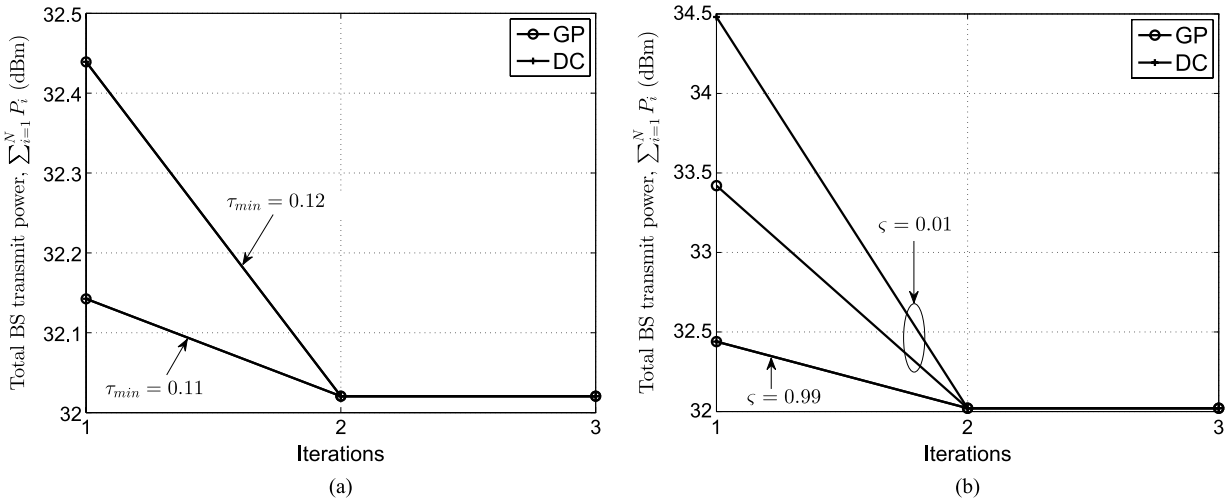

Fig. 6. Convergence of Algorithms 2 and 3 in Problem (P3) for AF relaying. (a) Fixed $\varsigma = 0.5$. (b) Fixed $\tau_{\min} = 0.12$.

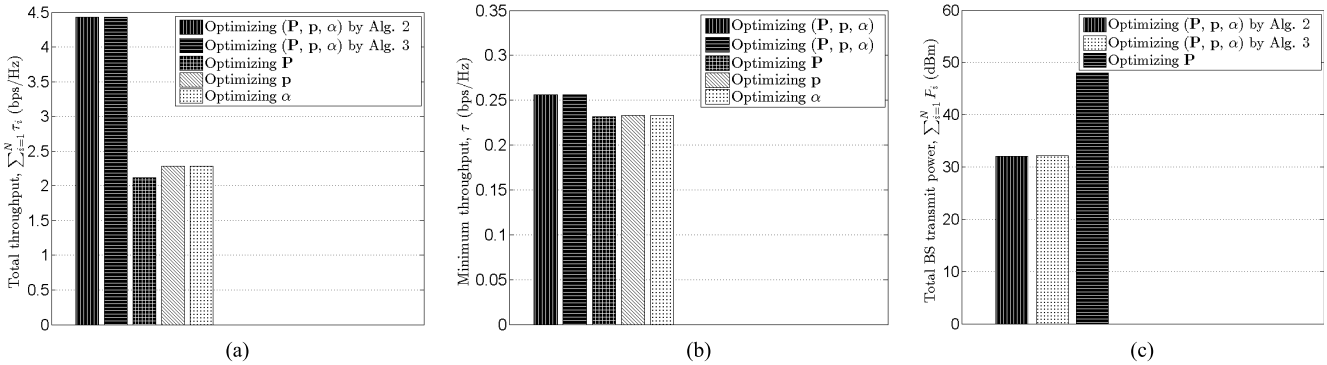

Fig. 7. Performance comparison of the proposed joint optimization algorithms and the separate optimization approaches. (a) Total throughput in Problem (P1). (b) Minimum throughput in Problem (P2). (c) Total transmit power in Problem (P3).

B. Importance of the Proposed Joint Optimization Algorithms for AF Relaying

Fig. 7 demonstrates the advantages of jointly optimizing $(\mathbf{P}, \mathbf{p}, \boldsymbol{\alpha})$ as in Algorithms 2 and 3 over optimizing those three parameters individually. In the latter approach, we only optimize one parameter (i.e., $\mathbf{P}$ or $\mathbf{p}$ or $\boldsymbol{\alpha}$) while fixing the remaining two parameters where applicable as $P_i = P_{\max};\ p_i = \eta\alpha_i \sum_{j=1}^{N} P_j;\ \alpha_i = 0.5\ \forall i \in \mathcal{N}$. Note that for the total power minimization problem (P3), $\mathbf{P}$ is optimized while $\mathbf{p}$ and $\boldsymbol{\alpha}$ must be fixed. Furthermore, in the individual optimization approach, we only present the results of GP-based solutions because both GP and DC approaches achieve similar outcomes.

The results presented in Fig. 7 have been averaged over 1000 independent simulation runs, and we set $\varsigma = 0.5$ and $P_{\max} = 46$ dBm. As expected, the proposed joint optimization algorithms outperform the sole optimization approach in all cases. The significant gain is observed in Fig. 7(a), where the total throughput is increased by 94%. Regarding Problem (P2), Fig. 7(b) shows that the minimum throughput in Problem (P2) is increased by 10% with the proposed Algorithms 2 and 3. The performance improvement is less pronounced here. This is because since the max-min fairness problem (P2) deals with the most disadvantaged cell-edge user, it is more difficult to support the QoS requirements of such a user compared with only maximizing the overall network performance. Finally, with the minimum throughput $\tau_{\min} = 0.12$ required by the most disadvantaged user in Problem (P3), Fig. 7(c) shows that the proposed algorithms reduce the total BS transmit power by 12 dB, i.e., almost 40 times over optimizing $\mathbf{P}$ alone.

C. Comparison of AF and DF Relaying

Fig. 8 plots the average sum throughput against different values of $P_{\max} = \{35, 37, 39, 41, 43, 45\}$ dBm obtained by the proposed joint optimization algorithm, while solving Problem (P1) for AF and DF relaying. The results for DF relaying include both the equal timeslot case, i.e., $\epsilon = \bar{\epsilon} = 0.5$, and the optimized ϵ case. With the equal timeslot assumption for BS-to-relay and relay-to-user transmissions, i.e., $\epsilon = \bar{\epsilon} = 0.5$, DF relaying increases the throughput by 33% at $P_{\max} = 35$ dBm. With an optimized value of ϵ, the throughput enhancement can be as high as 170% at $P_{\max} = 35$ dBm.

IX. Conclusions and Future Research Directions

In this paper, we have considered the challenging problems for jointly optimizing the BS transmit power, the relay PS factors, and the relay transmit power in a multicell network. It is assumed here that the relay (operating in either AF mode or

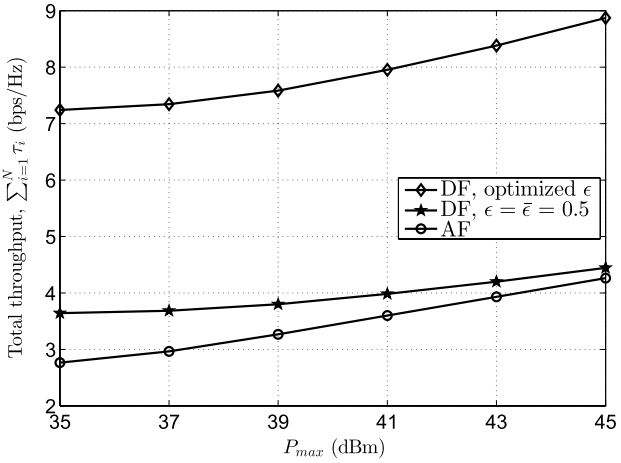

Fig. 8. Average sum throughput versus $P_{\min} = \{35, 37, 39, 41, 43, 45\}$ dBm of the proposed joint optimization algorithm [solving Problem (P1)] for AF and DF relaying. The results for DF relaying include both the fixed timeslot case, i.e., $\epsilon = \bar{\epsilon} = 0.5$, and the optimized ϵ case.

DF mode) is equipped with a PS receiver architecture that can split the received power to scavenge RF energy and to process the information signal from its respective BS. To resolve the highly nonconvex problem formulations, we have proposed SCA algorithms based on GP and DC programming that offer sum-throughput maximization, max-min throughput optimization, and sum-power minimization. We have proven that the devised algorithms converge to the solutions that satisfy the KKT conditions of the original nonconvex problems. Illustrative examples have demonstrated the clear advantages of our developed solutions.

In the case of multiple relays in a cell, two additional problems can be considered for future research: 1) in the first timeslot, beamforming design at the BS toward multiple relays; 2) in the second timeslot, relay selection to choose which relay to forward the BS message to which users and over which channel. While these problems are outside the scope of this paper, our proposed solution for the case of one relay and one user per cell can serve as a first building block toward joint design in more general cases.

REFERENCES

[1] J. Andrews *et al.*, "What will 5G be?" *IEEE J. Sel. Areas Commun.*, vol. 32, no. 6, pp. 1065–1082, Jun. 2014.

[2] I. Hwang, B. Song, and S. Soliman, "A holistic view on hyper-dense heterogeneous and small cell networks," *IEEE Commun. Mag.*, vol. 51, no. 6, pp. 20–27, Jun. 2013.

[3] Y. A. Sambo, M. Z. Shakir, K. A. Qaraqe, E. Serpedin, and M. A. Imran, "Expanding cellular coverage via cell-edge deployment in heterogeneous networks: Spectral efficiency and backhaul power consumption perspectives," *IEEE Commun. Mag.*, vol. 52, no. 6, pp. 140–149, Jun. 2014.

[4] D. L. Perez *et al.*, "Enhanced inter-cell interference coordination challenges in heterogeneous networks," *IEEE Trans. Wireless Commun.*, vol. 18, no. 3, pp. 22–30, Jun. 2011.

[5] Y. Yang, H. Hu, J. Xu, and G. Mao, "Relay technologies for WiMax and LTE-advanced mobile systems," *IEEE Commun. Mag.*, vol. 47, no. 10, pp. 100–105, Oct. 2009.

[6] R. Irmer *et al.*, "Coordinated multipoint: Concepts, performance, and field trial results," *IEEE Commun. Mag.*, vol. 49, no. 2, pp. 102–111, Feb. 2011.

[7] C. Yang, S. Han, X. Hou, and A. F. Molisch, "How do we design CoMP to achieve its promised potential?," *IEEE Wireless Commun. Mag.*, vol. 20, no. 1, pp. 67–74, Feb. 2013.

[8] X. Lu, P. Wang, D. Niyato, D. I. Kim, and Z. Han, "Wireless networks with RF energy harvesting: A contemporary survey," *IEEE Commun. Surveys Tuts.*, vol. 17, no. 2, pp. 757–789, 2nd Quart. 2014.

[9] H. Tabassum, E. Hossain, A. Ogundipe, and D. I. Kim, "Wireless-powered cellular networks: Key challenges and solution techniques," *IEEE Commun. Mag.*, vol. 53, no. 6, pp. 63–71, Jun. 2015.

[10] K. Huang and X. Zhou, "Cutting the last wires for mobile communications by microwave power transfer," *IEEE Commun. Mag.*, vol. 53, no. 6, pp. 86–93, Jun. 2015.

[11] Z. Ding, S. M. Perlaza, I. Esnaola, and H. V. Poor, "Power allocation strategies in energy harvesting wireless cooperative networks," *IEEE Trans. Wireless Commun.*, vol. 13, no. 2, pp. 846–860, Feb. 2014.

[12] Z. Ding, I. Krikidis, B. Sharif, and H. Poor, "Wireless information and power transfer in cooperative networks with spatially random relays," *IEEE Trans. Wireless Commun.*, vol. 13, no. 8, pp. 4440–4453, Aug. 2014.

[13] Z. Ding and H. Poor, "Cooperative energy harvesting networks with spatially random users," *IEEE Signal Process. Lett.*, vol. 20, no. 12, pp. 1211–1214, Dec. 2013.

[14] K. Cumanan, Y. Rahulamathavan, S. Lambotharan, and Z. Ding, "MMSE-based beamforming techniques for relay broadcast channels," *IEEE Trans. Veh. Technol.*, vol. 62, no. 8, pp. 4045–4051, Oct. 2013.

[15] A. A. Nasir, X. Zhou, S. Durrani, and R. A. Kennedy, "Relaying protocols for wireless energy harvesting and information processing," *IEEE Trans. Wireless Commun.*, vol. 12, no. 7, pp. 3622–3636, Jul. 2013.

[16] A. A. Nasir, X. Zhou, S. Durrani, and R. A. Kennedy, "Throughput and ergodic capacity of wireless energy harvesting based DF relaying network," in *Proc. IEEE ICC*, Sydney, NSW, Australia, 2014, pp. 4066–4071.

[17] A. A. Nasir, X. Zhou, S. Durrani, and R. A. Kennedy, "Wireless-powered relays in cooperative communications: Time-switching relaying protocols and throughput analysis," *IEEE Trans. Commun.*, vol. 63, no. 5, pp. 1607–1622, May 2015.

[18] K. Huang and E. Larsson, "Simultaneous information and power transfer for broadband wireless systems," *IEEE Trans. Signal Process.*, vol. 61, no. 23, pp. 5972–5986, Dec. 2013.

[19] W. Wang, L. Li, Q. Sun, and J. Jin, "Power allocation in multiuser MIMO systems for simultaneous wireless information and power transfer," in *Proc. IEEE VTC-Fall*, Las Vegas, NV, USA, 2013, pp. 1–5.

[20] D. W. K. Ng and R. Schober, "Resource allocation for coordinated multipoint networks with wireless information and power transfer," in *Proc. IEEE GLOBECOM*, Austin, TX, USA, Dec. 2014, pp. 4281–4287.

[21] L. Venturino, N. Prasad, and X. Wang, "Coordinated scheduling and power allocation in downlink multicell OFDMA networks," *IEEE Trans. Veh. Technol.*, vol. 58, no. 6, pp. 2835–2848, Jul. 2009.

[22] N. Ksairi, P. Bianchi, and P. Ciblat, "Nearly optimal resource allocation for downlink OFDMA in 2-D cellular networks," *IEEE Trans. Wireless Commun.*, vol. 10, no. 7, pp. 2101–2115, Jul. 2011.

[23] H. Chen, Y. Jiangy, Y. Li, Y. Ma, and B. Vucetic, "Distributed power splitting for SWIPT in relay interference channels using game theory," *IEEE Trans. Wireless Commun.*, vol. 14, no. 1, pp. 410–420, Jan. 2015.

[24] X. Zhou, R. Zhang, and C. K. Ho, "Wireless information and power transfer: Architecture design and rate–energy tradeoff," *IEEE Trans. Commun.*, vol. 61, no. 11, pp. 4754–4767, Nov. 2013.

[25] A. A. Nasir, D. T. Ngo, X. Zhou, R. A. Kennedy, and S. Durrani, "Sum throughput maximization for heterogeneous multicell networks with RF-powered relays," in *Proc. IEEE ICC*, London, U.K., Jun. 2015, pp. 3808–3814.

[26] M. Razaviyayn, M. Hong, and Z.-Q. Luo, "A unified convergence analysis of block successive minimization methods for nonsmooth optimization," *SIAM J. Optim.*, vol. 23, no. 2, pp. 1126–1153, 2013.

[27] J. Papandriopoulos and J. S. Evans, "SCALE: A low-complexity distributed protocol for spectrum balancing in multiuser DSL networks," *IEEE Trans. Inf. Theory*, vol. 55, no. 8, pp. 3711–3724, Aug. 2009.

[28] M. Chiang, C. W. Tan, D. P. Palomar, D. O'Neill, and D. Julian, "Power control by geometric programming," *IEEE Trans. Wireless Commun.*, vol. 6, no. 7, pp. 2640–2651, Jul. 2007.

[29] H. H. Kha, H. D. Tuan, and H. H. Nguyen, "Fast global optimal power allocation in wireless networks by local D.C. programming," *IEEE Trans. Wireless Commun.*, vol. 11, no. 2, pp. 510–515, Feb. 2012.

[30] D. T. Ngo, S. Khakurel, and T. Le-Ngoc, "Joint subchannel assignment and power allocation for OFDMA femtocell networks," *IEEE Trans. Wireless Commun.*, vol. 13, no. 1, pp. 342–355, Jan. 2014.

[31] L. Liu, R. Zhang, and K. C. Chua, "Wireless information and power transfer: A dynamic power splitting approach," *IEEE Trans. Commun.*, vol. 61, no. 9, pp. 3990–4001, Sep. 2013.

[32] B. R. Marks and G. P. Wright, "A general inner approximation algorithm for nonconvex mathematical programs," *Oper. Res.*, vol. 26, no. 4, pp. 681–683, Jul./Aug. 1978.
[33] S. Boyd and L. Vandenberghe, *Convex Optimization*. Cambridge, U.K.: Cambridge Univ. Press, 2004.
[34] P. Gahinet, A. Nemirovski, A. J. Laub, and M. Chilali, *LMI Control Toolbox User's Guide*. Natick, MA, USA: MathWorks, 1995, Mathworks Partner Series.
[35] N. Moller, "On Schoonhage's algorithm and subquadratic integer GCD computation," *Math. Comput.*, vol. 77, pp. 589–607, Jan. 2008.
[36] D. Karolak, T. Taris, Y. Deval, J. B. Begueret, and A. Mariano, "Design comparison of low-power rectifiers dedicated to RF energy harvesting," in *Proc. IEEE ICECS*, Seville, Spain, 2012, pp. 524–527.
[37] "Radio Frequency (RF) Requirements for LTE pico Node B," ETSI, Sophia-Antipolis Cedex, France, Tech. Rep. ETSI TR 136 931 V9.0.0, May 2011.
[38] M. Grant and S. Boyd, "CVX: Matlab software for disciplined convex programming, version 2.1," CVX Res., Austin, TX, USA, Mar. 2014. [Online] Available: http://cvxr.com/cvx
[39] M. Grant and S. Boyd, "Graph implementations for nonsmooth convex programs," in *Recent Advances in Learning and Control*, V. Blondel, S. Boyd, and H. Kimura, Eds. New York, NY, USA: Springer-Verlag, 2008, pp. 95–110, ser. Lecture Notes in Control and Information Sciences. [Online]. Available: http://stanford.edu/boyd/graph_dcp.html

Ali Arshad Nasir (S'09–M'13) received the Ph.D. degree in telecommunications engineering from the Australian National University (ANU), Canberra, ACT, Australia, in 2013.

He is an Assistant Professor with the School of Electrical Engineering and Computer Science, National University of Sciences and Technology, Islamabad, Pakistan. From 2012 to 2015, he was a Research Fellow with the ANU. His research interest includes signal processing in wireless communication systems.

Dr. Nasir received an ANU International Ph.D. scholarship and an ANU Vice Chancellor's Higher Degree Research travel grant in 2011. He is an Associate Editor of the IEEE CANADIAN JOURNAL OF ELECTRICAL AND COMPUTER ENGINEERING.

Duy Trong Ngo (S'08–M'15) received the B.Eng. degree (with First-Class Honors and the University Medal) in telecommunication engineering from the University of New South Wales, Sydney, NSW, Australia, in 2007; the M.Sc. degree in electrical engineering (communication) from the University of Alberta, Edmonton, AB, Canada, in 2009; and the Ph.D. degree in electrical engineering from McGill University, Montreal, QC, Canada, in 2013.

Since 2013, he has been a Lecturer with the School of Electrical Engineering and Computer Science, The University of Newcastle, Callaghan, NSW, Australia. His research interest includes radio resource allocation for wireless communication systems.

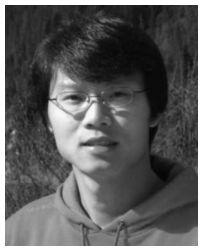

Xiangyun Zhou (M'11) received the Ph.D. degree in telecommunications engineering from the Australian National University (ANU), Canberra, ACT, Australia, in 2010.

He is a Senior Lecturer with the ANU. His research interests include communication theory and wireless networks.

Dr. Zhou currently serves on the Editorial Board of the IEEE TRANSACTIONS ON WIRELESS COMMUNICATIONS and the IEEE COMMUNICATIONS LETTERS. He also served as a Guest Editor for the IEEE COMMUNICATIONS MAGAZINE's feature topic on wireless physical-layer security in 2015. He was a Cochair of the IEEE International Conference on Communications (ICC) Workshop on Wireless Physical Layer Security at ICC'14 and ICC'15. He was the Chair of the ACT Chapter of the IEEE Communications Society and the IEEE Signal Processing Society from 2013 to 2014. He received the Best Paper Award at ICC'11.

Rodney A. Kennedy (S'86–M'88–SM'01–F'05) received the B.E. degree from the University of New South Wales, Sydney, NSW, Australia, in 1982; the M.E. degree from The University of Newcastle, Callaghan, NSW, in 1985; and the Ph.D. degree from the Australian National University (ANU), Canberra, ACT, Australia, in 1989.

He is currently a Professor with the Research School of Engineering, ANU. His research interests include digital signal processing, digital and wireless communications, and acoustical signal processing.

Salman Durrani (S'00–M'05–SM'10) received the Ph.D. degree in electrical engineering from the University of Queensland, Brisbane, QLD, Australia, in 2004.

He is a Senior Lecturer with the Australian National University, Canberra, ACT, Australia. His research interests include wireless communications and signal processing.

Dr. Durrani currently serves as an Editor for the IEEE TRANSACTIONS ON COMMUNICATIONS and the Chair of the ACT Chapter of the IEEE Signal Processing Society and the IEEE Communications Society. He is a member of Engineers Australia and a Senior Fellow of The Higher Education Academy, U.K.